AFRL-RX-WP-TP-2010-4152

MODELING OF RESIDUAL STRESS AND MACHINING DISTORTION IN AEROSPACE COMPONENTS (PREPRINT)

Kong Ma and Robert Goetz

Rolls-Royce Corporation

Shesh K. Srivatsa

GE Aviation

MARCH 2010

Approved for public release; distribution unlimited.

See additional restrictions described on inside pages

STINFO COPY

AIR FORCE RESEARCH LABORATORY
MATERIALS AND MANUFACTURING DIRECTORATE
WRIGHT-PATTERSON AIR FORCE BASE, OH 45433-7750
AIR FORCE MATERIEL COMMAND
UNITED STATES AIR FORCE

REPORT DOCUMENTATION PAGE

Form Approved
OMB No. 0704-0188

The public reporting burden for this collection of information is estimated to average 1 hour per response, including the time for reviewing instructions, searching existing data sources, gathering and maintaining the data needed, and completing and reviewing the collection of information. Send comments regarding this burden estimate or any other aspect of this collection of information, including suggestions for reducing this burden, to Department of Defense, Washington Headquarters Services, Directorate for Information Operations and Reports (0704-0188), 1215 Jefferson Davis Highway, Suite 1204, Arlington, VA 22202-4302. Respondents should be aware that notwithstanding any other provision of law, no person shall be subject to any penalty for failing to comply with a collection of information if it does not display a currently valid OMB control number. **PLEASE DO NOT RETURN YOUR FORM TO THE ABOVE ADDRESS**.

1. REPORT DATE *(DD-MM-YY)*	2. REPORT TYPE	3. DATES COVERED *(From - To)*
March 2010	Technical Paper Preprint	01 March 2010 – 01 March 2010

4. TITLE AND SUBTITLE
MODELING OF RESIDUAL STRESS AND MACHINING DISTORTION IN AEROSPACE COMPONENTS (PREPRINT)

5a. CONTRACT NUMBER
In-house

5b. GRANT NUMBER

5c. PROGRAM ELEMENT NUMBER
62102F

6. AUTHOR(S)
Kong Ma and Robert Goetz (Rolls-Royce Corporation)
Shesh K. Srivatsa (GE Aviation)

5d. PROJECT NUMBER
4347

5e. TASK NUMBER
RG

5f. WORK UNIT NUMBER
M02R1000

7. PERFORMING ORGANIZATION NAME(S) AND ADDRESS(ES)
Rolls-Royce Corporation
Indianapolis, IN

GE Aviation
Cincinnati, OH

8. PERFORMING ORGANIZATION REPORT NUMBER
AFRL-RX-WP-TP-2010-4152

9. SPONSORING/MONITORING AGENCY NAME(S) AND ADDRESS(ES)
Air Force Research Laboratory
Materials and Manufacturing Directorate
Wright-Patterson Air Force Base, OH 45433-7750
Air Force Materiel Command
United States Air Force

10. SPONSORING/MONITORING AGENCY ACRONYM(S)
AFRL/RXLMD

11. SPONSORING/MONITORING AGENCY REPORT NUMBER(S)
AFRL-RX-WP-TP-2010-4152

12. DISTRIBUTION/AVAILABILITY STATEMENT
Approved for public release; distribution unlimited.

13. SUPPLEMENTARY NOTES
Chapter submitted for publication in the American Society for Metals (ASM) Handbook. PAO Case Number: 88ABW-2010-1307; Clearance Date: 18 Mar 2010.

This work was funded in whole or in part by the Department of the Air Force. The U.S. Government has for itself and others acting on its behalf an unlimited, paid-up, nonexclusive, irrevocable worldwide license to use, modify, reproduce, release, perform, display, or disclose the work by or on behalf of the U.S. Government. Paper contains color.

14. ABSTRACT
The insertion of new materials into aircraft systems takes several years and many millions of dollars. Experimental trials to define the manufacturing process to meet the specifications can add significant time and cost. Many military programs have small lot production in either initial engine development programs or specialized production, providing additional criticality to improving the "First Time Yield" (FTY) of manufacturing processes, and quickly resolving production issues. Additionally, the impact of an unintended process change is unknown without evaluating the component, again adding time and cost to issue resolution. Therefore, new approaches are required to facilitate the rapid certification of materials and processes technologies. Significant improvements in manufacturing processes have been realized by process modeling tools such as DEFORM™ and FORGE for metal forming and Procast™ for casting, which are now in routine industrial use.

15. SUBJECT TERMS
"First Time Yield" (FTY), DEFORM™ and FORGE

16. SECURITY CLASSIFICATION OF:			17. LIMITATION OF ABSTRACT:	18. NUMBER OF PAGES	19a. NAME OF RESPONSIBLE PERSON (Monitor)
a. REPORT	b. ABSTRACT	c. THIS PAGE			Christopher F. Woodward
Unclassified	Unclassified	Unclassified	SAR	48	19b. TELEPHONE NUMBER *(Include Area Code)* N/A

Standard Form 298 (Rev. 8-98)
Prescribed by ANSI Std. Z39-18

MODELING OF RESIDUAL STRESS AND MACHINING DISTORTION IN AEROSPACE COMPONENTS

Kong Ma, Robert Goetz
Rolls-Royce Corporation, Indianapolis, IN

Shesh K Srivatsa
GE Aviation, Cincinnati, OH

1.0 INTRODUCTION

1.1 Technical Need

The insertion of new materials into aircraft systems takes several years and many millions of dollars. Experimental trials to define the manufacturing process to meet the specifications can add significant time and cost. Many military programs have small lot production in either initial engine development programs or specialized production, providing additional criticality to improving the "First Time Yield" (FTY) of manufacturing processes, and quickly resolving production issues. Additionally, the impact of an unintended process change is unknown without evaluating the component, again adding time and cost to issue resolution. Therefore, new approaches are required to facilitate the rapid certification of materials and processes technologies. Significant improvements in manufacturing processes have been realized by process modeling tools such as DEFORM™ and FORGE for metal forming and Procast™ for casting, which are now in routine industrial use. Modeling and simulation are critical for increasing the affordability of current and future aerospace materials and products and in developing and certifying materials in a shorter timeframe that more closely matches the product design cycle.

Aircraft engine and airframe structural components that are machined from forgings or plate stock represent a significant cost of both military and commercial aircraft. Typical component applications, as shown in Figure 1, are rotating disks in aircraft engines and structural components in airframes. The buy-to-fly weight ratio, which is the ratio of the forged material weight to the finished component weight, is typically between 4 and 10 for such components. The excess material is removed by various machining operations, which are a major contributor to the cost of forged components.

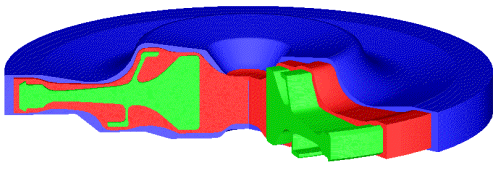

(a) Typical aircraft engine forging.

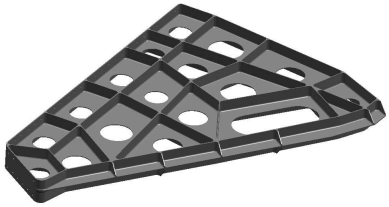

(b) Typical airframe structural forging.

Blue: forging shape
Red: intermediate shape
Green: finish machined shape
Large volume of material machined away.

Intricate geometrical features result in a large volume of material being machined away.

Figure 1. Aircraft engine and airframe components with large "Buy-to-Fly" ratios and high machining costs.

Metallic components undergo various forming processes such as casting, forging, rolling, etc., in which the material is heated to very high temperatures. A typical wrought component of a titanium or nickel based alloy begins as an ingot, the cast structure is broken down into billet form, which is then forged into the rough shape of the component with positive stock surrounding the finished shape. Deformation occurring during the forming process causes residual stresses which can be compounded by thermal gradients. After forming, the components are subjected to a series of heat treatment processes to improve the microstructure and material properties (e.g., toughness, strength, creep, fatigue). Most heat treatment processes involve heating the material to a very high temperature in order to produce a change in microstructure (e.g., phase transformation, recrystallization).

Nickel base superalloy disks used in aircraft engines typically undergo a two-step heat treatment process, solution and age. The first step is a solution treatment, and the solution temperatures are often high enough (~2000^{o}F or ~1100^{o}C, depending on the alloy) to completely relax any pre-existing residual stress induced during the forming process. When the components are removed from the heat treat furnace at the end of the heating and soaking process, they are transported to the quenching station, during which the components lose heat to the ambient: radiation to the surrounding surfaces, natural convection through air, and conduction to the handling mechanism through the direct contact areas. This period is called the quench delay or transfer time and usually is very short (15 – 60 seconds).

This is followed by rapid quenching. When the component is subjected to the much cooler quench media (typically oil, water, polymer, salt, or forced air) the outer surface of the component cools down rapidly, contracts, and metallurgically stabilizes when it reaches a relatively low temperature (e.g., below 900^{o}F, or 480^{o}C for nickel alloys) while the interior is still at a high temperature. At this point, the outside of the component is under tensile stress and yields while the interior material is under compression because the outer volume cannot contract (inward) against the yet to contract hot interior. Gradually the heat from the inside dissipates outward, the interior material then tries to contract but now the outer volume is already relatively fixed since it is at a much lower temperature. Therefore, the interior is under tension and the outer region is under compression because it is being pulled inward by the inner material. Plastic deformation subsequent to yielding induces bulk residual stresses in all directions.

Temperature gradients during quenching cause thermal stresses which drive localized plastic deformation and residual stress build-up. Upon cooling to room temperature, residual stresses can exceed half of the alloy tensile strength. Often, to obtain favorable material strength and microstructure, fast cooling (quenching) is applied. Higher cooling rates result in higher residual stresses. Residual stresses resulting from thermo-mechanical processing can cause in-process cracking, machining distortion, in-service distortion, and/or lowered life.

The stress profile within a component depends on the local geometry features and the temperature difference between the near surface area and the quench media (which determines the rate of heat loss). A thinner cross section area usually has lower stress than a thicker section. Variations in residual stress occur due to variability in manufacturing process conditions, e.g. the loading pattern of components in the furnace and quench media, the agitation level in quench tanks, and the nature of the heat treat fixtures.

During the second heat treatment step, aging, the component is reheated to a temperature much lower than the solution temperature (typically 1200-1500^{o}F or 650-820^{o}C) to form secondary and tertiary gamma prime in nickel base superalloys. This step completes the transformation to a desired microstructure and

properties with the added benefit of stress relaxation through creep and recovery processes. The amount of stress relaxation depends on the time and temperature of the age cycle, and the magnitude of the initial residual stress. Higher temperatures result in a greater degree of relaxation. Stress relaxation is related to the creep behavior of the material, and therefore the microstructure (grain size and gamma prime) also affects stress relaxation. If the level of residual stress is below the steady state relaxation stress, further relaxation will not occur unless higher temperatures are used. Thus residual stress cannot be eliminated, only reduced during final aging, and the component still has enough residual stress to affect its behavior during machining and in service.

Component distortion can be caused by material bulk stresses resulting from heat treating operations and/or by local near-surface machining induced stresses. When the component cross section is thick, bulk residual stresses dictate component distortion. As the cross section is machined thinner (~0.125" or 3 mm), surface residual stress begins to play a more significant role in component distortion.

The prediction of residual stresses at quantified levels of uncertainty can improve processing methods, component design, robustness, performance and quality and achieve more efficient material utilization and aircraft system efficiency which result in lower environmental impact. Distortion of machined titanium and nickel alloys contributes significantly to the cost of these components. Heat treatment and machining are the two critical operations in the manufacture of engine and airframe components which influence residual stress. Residual stresses and associated distortion have a significant effect upon manufacturing cost in four distinct ways.

First, the forging and intermediate heat treat shapes contain additional material to account for expected distortion (Figure 2). This material, added to assure a positive material envelope over the finished component shape, represents a raw material cost and increases the machining cost. This also imposes a limit on the benefit of near-net-shape forging which is being pursued vigorously by the industry.

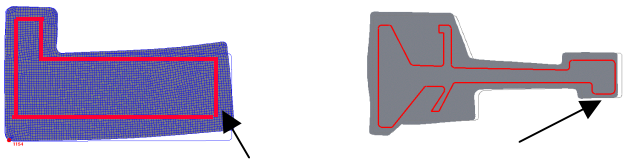

Figure 2. Extra material envelope is needed to compensate for distortions during heat treat and machining to the inside finished component shape.

Second, component distortion during machining requires that the machining process engineer plan machining operations and fixtures so that distortion does not compromise the finished component shape. Distortion during and after machining can result in added operations, line-up and straightening, rework or scrap. Typically additional machining operations and setups are added in a time-consuming and costly trial-and-error approach to minimize the effects of component distortion. For example, components such as disks are machined alternately on either side in an attempt to stepwise balance the distortion. The time spent "flipping" components erodes productivity for thick, stiff components; for thin components the strategy may be inadequate.

Third, residual stresses and associated distortion add complexity to machining process development and shop operations. Distortion affects the details of the machining plan and the way the component interfaces with machining fixtures. These effects generally vary between material suppliers, from lot-to-lot and from one machining process to another. Distortion thereby not only influences the effort incurred during initial development of machining plans but may require adjustments after the initial plan has been set.

Finally, distortion results in preload of aircraft structures and fasteners and can cause assembly problems. Manufacturing residual stresses can adversely impact the behavior of the components during service. Distorted and pre-stressed components can result in fatigue capability degradation by increasing the local mean stresses. Residual stresses affect the dimensional stability of rotating components in aircraft engines. These components are exposed to high temperatures for long times and distortions can effect system tolerances, clearances, and efficiency. For an accurate analysis of component behavior during service, the manufacturing residual stresses must be included as initial conditions.

The physics and mathematics of residual stress redistribution within a component during machining are well understood. Determining residual stresses and subsequent distortion requires modeling using finite element methods (FEM). This method has been used to evaluate the effect of processing conditions upon residual stress development and the effect of residual stresses upon distortion during machining. The build-up of residual stresses during heat treatment, the machining process imparted residual stresses, and the subsequent relaxation following metal removal are difficult to assess using intuition, engineering judgment, or empirical methods. The physical interplay of quench heat transfer, elevated temperature mechanical behavior, and localized plastic deformation is complex. Subtle changes in processing conditions and component geometry can significantly affect the magnitude and pattern of residual stresses.

For routine use, a fast-acting validated physics-based model with sufficient fidelity and robustness is needed to accurately predict the effects of thermo-mechanical processing and reduce scatter in residual stress, microstructure, mechanical properties, and their measurement. Residual stress modeling technology needs to be standardized to meet an industry requirement for accuracy and capability in manufacturing (distortions), service (dimensional stability), lifing (fatigue life, crack initiation, crack growth and propagation), and material testing (measurement scatter and sampling effects).

There is a need to understand the effects of heat treating and machining on distortion and to predict, minimize, and control these distortion-related processes to achieve robust six-sigma quality. There is a need to develop heat treatment and machining processes for minimizing distortions realizing that this is not always the same as minimizing residual stresses. In addition, there is a need to accurately predict residual stress and consider its impact on component life and behavior in service. The industrial drive is towards stronger and longer lasting components with higher temperature capability. As new materials with better properties to meet more exacting requirements are introduced, they will be more difficult to machine. While material scientists are developing higher temperature materials, it is also feasible to "squeeze" more out of existing designs and materials by optimizing the fabrication process and the component design. One way to improve component design and increase life is by understanding the distribution of residual stress from the manufacturing process and linking it with the product life cycle. Modeling will help reduce machining problems and thereby enable more rapid introduction of high performance materials and components.

1.2 Objectives of Residual Stress and Machining Distortion Modeling

The overall objective is to develop and validate a high productivity modeling method that accurately predicts the magnitude and pattern of distortion during machining of forgings used in aircraft engines and airframe structures and establish an approach for using machining modeling to generate machining plans that yield less component distortion and reduce the cost of machining.

1.3 MAI Programs

For almost a decade the USAF Metals Affordability Initiative (MAI) has devoted significant resources to understanding the impact of residual stresses upon component variability and machining distortion. The MAI team consists of materials developers, forgers, software developers, universities, aircraft engine makers and airframers to bring the real world perspectives of the entire supply chain to the project. The methods developed represent a sound engineering practice for predicting machining distortion and are

available for licensing in commercial codes. Many aerospace OEMs and their suppliers now have established in-house analysis methods. The MAI projects have reduced the time-to-implementation of the process technology by permitting a focused, larger scale, complete effort across engine manufacturers, air framers and material and machining suppliers than would be possible if efforts were conducted by individual companies alone.

Significant progress was made in the development and validation of 2-D modeling tools for predicting machining distortions in the USAF MAI, Dual Use Science and Technology (DUST-7) Program, Cooperative Agreement No. F33615-99-2-5216. This program advanced the state-of-the-art in going from the previous state of a time-consuming, manual, partially validated, not production ready procedure to an automated, high productivity, user-friendly, fast-acting, validated, commercially supported, and production ready analysis tool which can be used to achieve significant cost savings. It was shown that 2-D distortions can be predicted to within the typical process variability of $\pm$ 20 % or $\pm$ 5 mils (0.125 mm).

Aircraft engine rotating components are 2-D axi-symmetric up until the final machining operations when 3-D features such as dovetail slots, cooling holes, etc. are machined. For this reason and because of the simpler nature of 2-D models as compared to 3-D, the development of 2-D tools was addressed first. The 2-D model was rigorously validated first on simple shaped forgings and later for complex shapes in a production environment. 2-D rotating disks account for majority of aircraft engine forgings. The machining model developed realistically captures the process boundary conditions (tooling constraints) for any user-specified sequence of machining operations. The method was rigorously validated first on simple shapes in a well-controlled situation and then extended to complex shapes in a production environment. The material chosen for this program was Cast and Wrought U720 but the model/method is pervasive and can be employed for other materials.

The 2-D model has been implemented at various aircraft engine makers and it has been used successfully for many production components. This analytical tool guides machining operation sequence and tooling design for rotor hardware to minimize component distortion, which was before predominately an experienced based- trial and error process.

Following the successful completion of the 2-D program, the MAI team is developing 3-D distortion modeling tools which are described below. The results presented in this Chapter are largely based on the MAI programs.

2.0 MODELING OF HEAT TREAT INDUCED RESIDUAL STRESS

2.1 Finite Element Residual Stress Analysis

Residual stress analysis involves:

1) Determination of heat transfer coefficients during quenching.
2) Measurement of material constitutive behavior (elastic-plastic-creep) at processing conditions.
3) Finite element analysis to calculate thermal and stress fields.
4) Finite element analysis for machining distortion.
5) Finite element analysis for in-service distortion and for strength and lifing.

Commercially available process modeling tools, such as DEFORM™ by Scientific Forming Technology Corporation and FORGE by TRANSVALOR, are finite element based analysis tools. They employ an elastic-plastic formulation which is the necessary basis for the model formulation. The detailed steps of setting up a model for the heat treatment process vary depending on the software used. However, they all involve several general steps:

1) Construct the heat treat geometrical model from CAD tools.

2) Obtain the thermal-physical material properties for the component material. This includes thermal conductivity, heat capacity, density, thermal expansion coefficient, Young's modulus, and flow stress describing plastic behavior. All properties are temperature dependent and also depend on the microstructure and previous processing history of the material. The use of realistic material data is critical to the success of any modeling effort.

3) Obtain the detailed process information. This includes the heat treat solution temperature, soak time, quench delay time, quench media type, media temperature, component loading configuration, etc. Similar processing data is needed for any subsequent stress relief (or aging) processes.

4) Determine the heat transfer coefficients (HTC's) for the interface between the quenching media and the component. Using the analytical approach, one can use the sophisticated two phase (gaseous and liquid) flow computational fluid dynamic (CFD) methods to simulate the quenching agitation interacting with the specific component geometry. This requires very detailed characterization of the physical quenching configuration and is time consuming A much simpler approach is to experimentally determine the effective heat transfer coefficients by instrumenting an experimental component with thermo-couples. The HTC's are then input into the modeling software as time and temperature dependent boundary conditions.

5) Mesh the component geometry. All the general rules and guidelines used for standard finite element analysis apply to the process model, e.g., quad elements are better than triangular elements, a higher density mesh yields more accurate results, and so on. One point worth noting is that the elastic-plastic formulation is used to perform the thermal-mechanical analysis of components. Therefore, particular attention should be given to the mesh density in the areas subjected to steep thermal and mechanical changes during the heat treat cycle.

6) Run the heat treat model. Because of the complexity of the algorithm and the time and temperature base of the process model, it usually takes from a couple of hours for a mid size 2-D model to over a couple of days of a complex 3-D model. Like any finite element analysis, if the solution fails to converge, using smaller simulation time steps and/or altering the mesh can help eliminate the problem.

2.2 Modeling Procedures (2D)

Generally, three procedures have been commonly used to model the machining distortion (Figure 3). All these techniques use different methods on how the material is removed during machining and the subsequent re-equilibration of residual stresses. All the techniques described below neglect the surface residual stress induced by the interaction between the machine tool and the component, and therefore the effect of cutting conditions is also ignored. The effect of machining induced stresses is addressed in a later section in this chapter.

In the "One-Step" Procedure, plastic strains from the heat treat shape are mapped onto the machined shape, the strains and stresses are re-equilibrated to obtain the resulting distortion. In essence, this method means that all the material is machined off instantaneously in one machining pass. This method is straightforward and easy to implement; it avoids remeshing associated with modeling each machining operation; and it predicts bulk distortions and trends correctly. However, it ignores the influence of the machining path and the effect of in-process shape change on work-piece/fixture interface and its accuracy decreases with increasing distortion.

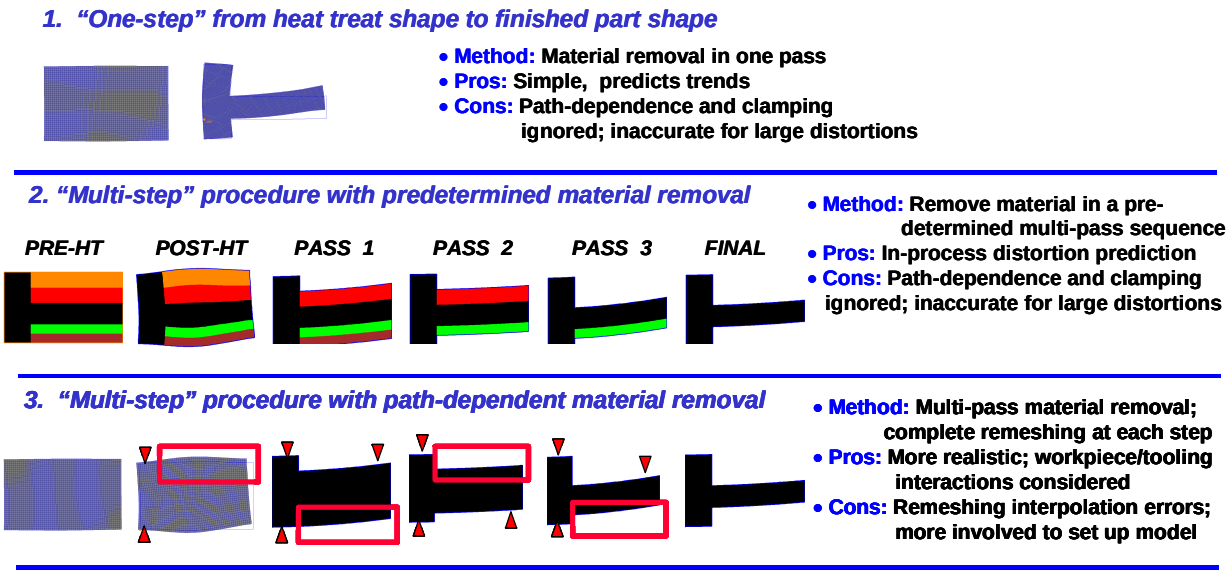

Figure 3. Comparison of different machining distortion prediction methods. The multi-step procedure with path-dependent material removal most accurately represents what is happening in practice.

The "Multi-Step" Procedure with predetermined material removal is similar to the one-step procedure, but material is removed in multiple passes based on a pre-determined machining sequence. The workpiece is meshed up-front to follow the machining sequence. This method also avoids remeshing associated with modeling each machining operation, and it predicts bulk distortions and trends correctly. However, it ignores the influence of the machining path and the effect of in-process shape change on work-piece/fixture interface and its accuracy decreases with increasing distortion. The initial meshing is more involved than the one-step method. If changes in machining sequences are to be evaluated, the heat treat analysis has to be completely redone.

In the "Multi-Step" procedure with path-dependent material removal, a complete remeshing is performed at each machining operation and the material removal follows the actual machining sequences. This is a more realistic representation of the machining process and it accounts for in-process distortions and workpiece/tooling interactions. It is most involved to setup the model. The material removal can be accomplished in two ways: Boolean or remeshing.

Boolean procedure (Figure 4 (a)): The material inside the machining path is removed to obtain the new geometry by a Boolean operation of the current geometry and the machining path. The new geometry follows the distorted geometry from the preceding step everywhere *except* where the machining cut is taken. This new geometry which represents the workpiece shape after machining, is remeshed, and the stresses/strains re-equilibrated to get the unrestrained distortion. When the Boolean cut is very thin (e.g., on the last pass), and the workpiece is not constrained during cutting, there will be very little additional distortion, and the cut face will follow the cutting tool path.

Remeshing Procedure (Figure 4 (b)): The plastic strains from the current geometry are mapped onto the machined geometry and the stresses re-equilibrated to obtain the resulting distortion. The new geometry follows what the user has pre-defined and not the distorted geometry from the previous step. The new geometry is indicated by the solid line. Remeshing to this new geometry causes the distortion from the preceding steps to be not carried through, as shown on the uncut faces in Figure 4 (b).

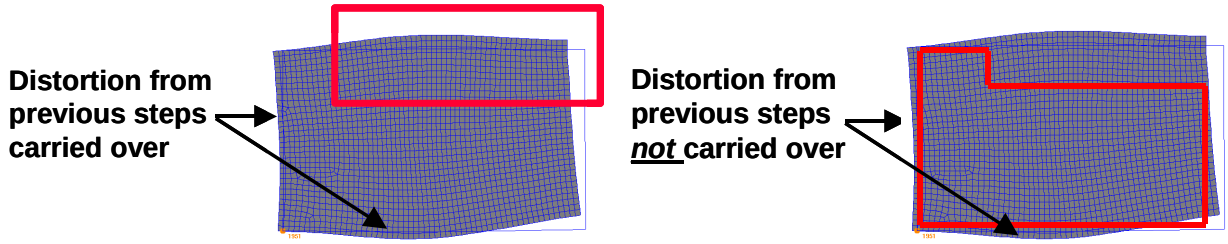

(a) Boolean Procedure (b) Remeshing Procedure

Figure 4. Boolean and Remeshing procedures.

Method 1 is straightforward, and Methods 2 and 3 require a large amount of user time to set up the problem for a general multi-step machining process. As a result, such analyses are not performed routinely. An automated version of Method 3 that minimizes model set up time, streamlines the overall procedure and minimizes the interpolation error was developed in the MAI programs.

2.3 Modeling Procedures (3D)

3-D distortion modeling is needed to address airframe structures and complex engine components. Figure 5 shows a distorted airframe component with a 3-D geometry. Figure 6 shows both axi-symmetric and non-axi-symmetric distortions of a nominally 2-D axi-symmetric shaped engine disk forging.

Figure 5. Distorted airframe component. This component was machined flat. The material stress and machining induced stress are causing it to distort.

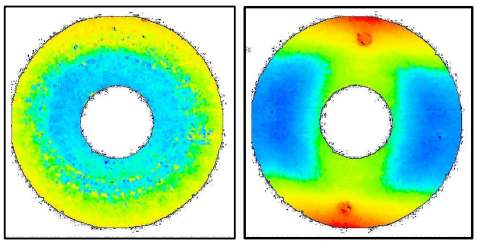

Figure 6. Optical scan pictures showing axi-symmetric and non-axi-symmetric distortion (due to non-axi-symmetric fixturing) following heat treatment. Colors indicate axial distortion.

In the modeling of the material removal process during machining, a new finite element mesh has to be generated on the as-machined shape. Residual stresses and strains have to be interpolated from the pre-machined shape (mesh) to the post-machined shape (mesh). This process of interpolation introduces errors in the simulation which can be significant if the component geometry has thin walls adjacent to thicker sections. This problem is more acute in 3-D modeling than in 2-D modeling because of the increased geometrical complexity of 3-D shapes (thin/thick sections) and because of the limitations on the fineness of the mesh that can be employed in 3-D to keep the computations manageable. The solution

accuracy was improved with a combination of controlling the local mesh density to have finer elements in thin geometrical features and high stress gradient regions, local remeshing, and improved interpolation schemes.

Local remeshing: During global remeshing, a completely new mesh is generated over the entire volume of the workpiece. Therefore, every element and node in the model is changed and the state variables are interpolated from the old mesh to the new mesh. This introduces large interpolation errors. During material removal, generally only a small volume of the workpiece geometry is altered. Figure 7 shows a schematic of the material removal process. In the local remeshing methodology, only the elements along the machined surface and their neighboring elements are remeshed. As compared with the original mesh, 86.7% nodes and 79.6% elements remain unchanged in this example. During data interpolation, only the modified nodes/elements are affected. Therefore, interpolation error can be avoided for the major part of the mesh which remains unchanged.

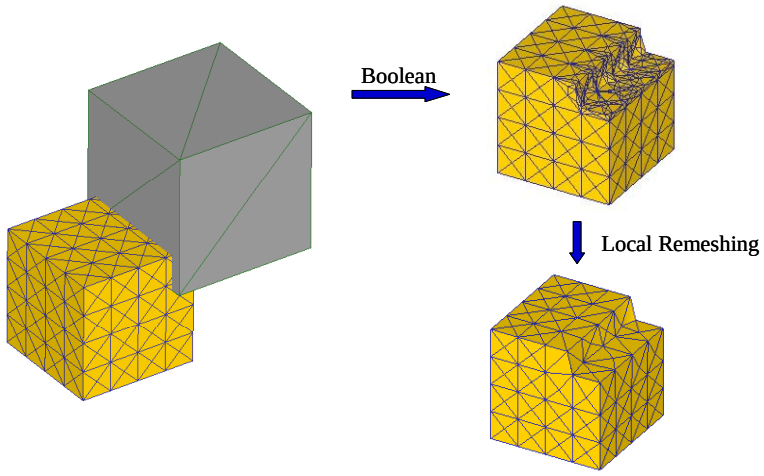

Figure 7. Local remeshing of elements affected by the machining process.

Two new interpolation schemes were developed. In the first, the interpolation is performed based on a local polynomial fit. In the second, the element variables are stored also at the nodes and the nodal values used during interpolation, which avoids the error during transfer of element data to nodes. The interpolation error was reduced significantly with the new interpolation schemes. When interpolating onto the same mesh the error in radial distortion was reduced to 2.5% as compared to 50% with the old method.

The method of combining local remeshing, improved interpolation, and mesh windows to control element size helps reduce errors. In general this method results in peak values of stress and strain being retained more accurately than the previous methods i.e., there is less smoothing error with the new method. Simulation results were found to be in good agreement with experimental data. All predictions were within 20% of the measurements with the new method.

In order to easily setup the model for multiple machining operations and passes, a template (Figure 8) was set up which can position the workpiece, the fixtures and loads, the material removal in a user-friendly setup. A preview of all the machining steps ensures error-free setup before the simulations are commenced.

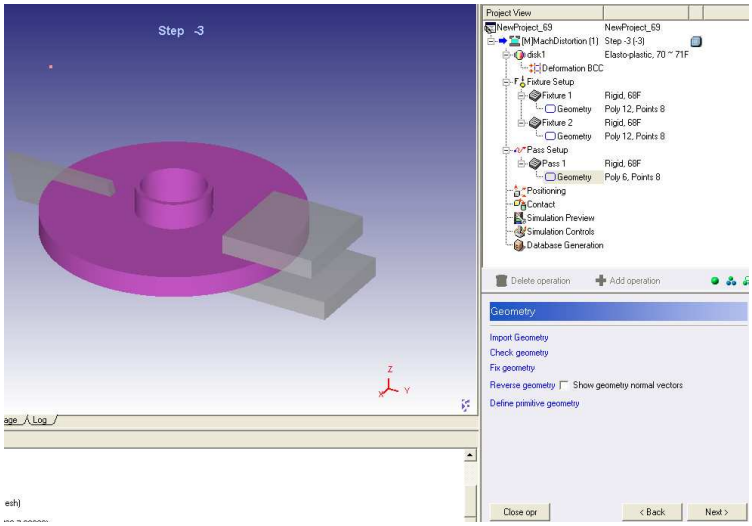

Figure 8. Machining distortion template.

In order to facilitate the material removal process for machining distortion modeling, the machining path information (described by G code) was converted to a geometry that can be used to generate the machined workpiece configuration (Figure 9). A G-code interpreter was developed and tested with several examples (Figure 10).

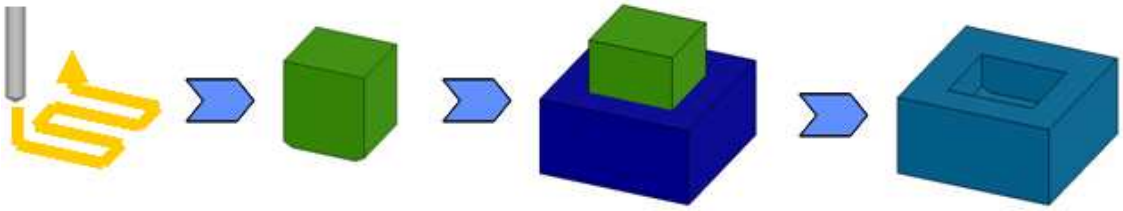

Figure 9. Boolean geometry creation from machining G code, material removal, and machined component.

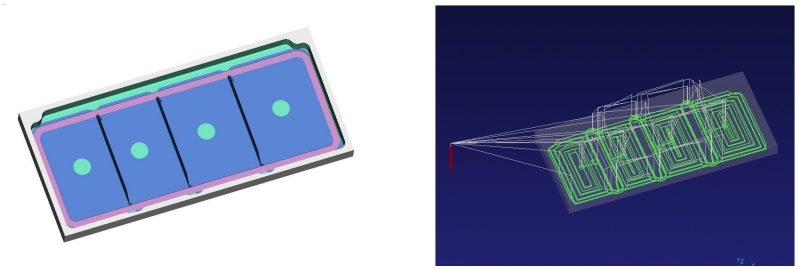

Figure 10. G-code converter: machining path (G-code) converted to material removal geometry.

During the simulation of residual stresses and machining distortions, it is necessary to constrain the 6 degrees of freedom in the workpiece to eliminate rigid body motion. Guidelines were developed on the selection of the nodes and the manner in which they need to be constrained. A pre-processing function was developed to automate/guide the definition of these boundary conditions. The method is:

1. Fix one node in x, y, z directions. This removes the three-degrees of freedom in translation.
2. Find a point at the same x and z but different y – fix this in z direction – removes x-rotation.
3. Find a point at the same y and x but different z – fix this in x direction – removes y rotation.

4. Find a point at the same z and y but different x – fix this in y direction – removes z rotation.

The machining distortion solution is dependent upon the chosen reference boundary conditions to constrain rigid body motion. A facility was developed to allow the user to easily select reference points/planes/axes to represent the predicted distortion in the selected frame of reference. This feature enables the display of the distortion solution in any frame of reference and enables easy comparison with measured data. In the free state distortion simulations, six degrees of freedom are removed by assigning boundary condition constrains to the model. Depending upon the locations where the boundary condition constraints are applied, the distortion results may appear to be different. For the 2-D example shown in Figure 11, the distortion results appear to be different with respect to where the constraints are applied. However, if the distorted models are rotated and translated appropriately, the distortion results would be the same. This means that results using different boundary condition constraints can be converted to the same results using a suitable reference frame definition. Various other improvements were made to facilitate the display of distortions in a easily usable format, e.g. axial runout display, etc.

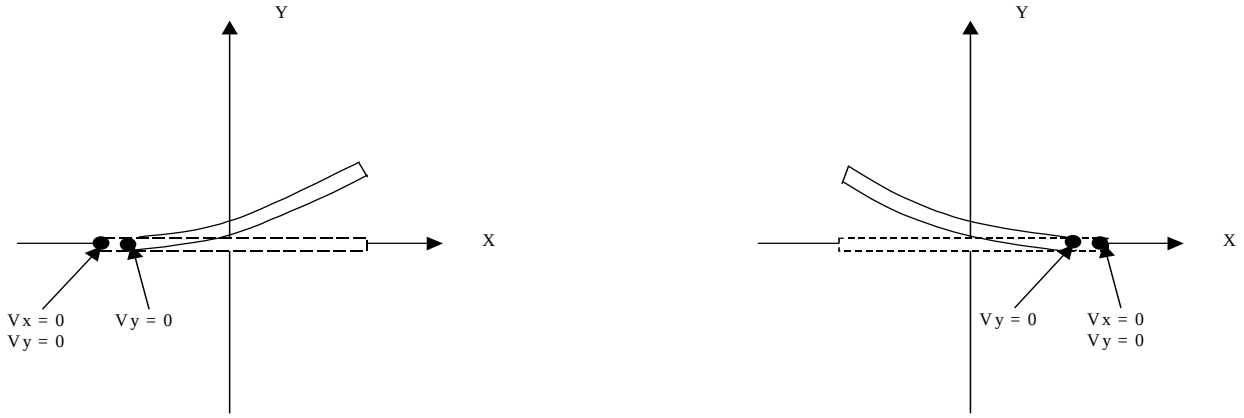

Figure 11. 2D illustration showing different distortion results using different constraints.

3.0 MODELING DATA REQUIREMENTS

3.1 Material Characterization

The MAI programs have focused on three materials: Ti-64, U720 and alloy 718. However, the model/method is pervasive and can be applied to other materials. The data needed in order to do this are listed below. All data should cover the range from room temperature up to the heat treat temperature.

- Constitutive behavior (stress-strain in plastic region)
- Young's Modulus
- Creep and stress relaxation data
- Poisson's Ratio
- Thermal Expansion Coefficient
- Heat Capacity
- Thermal Conductivity
- Heat transfer coefficients during the entire quench process

3.2 On-Cooling Tensile Tests

On-cooling tests are used to generate data describing the constitutive behavior of the material: stress as a function of strain, strain rate and temperature. Data should be generated at a minimum of two different strain rates. Details of the testing procedure are as follows:

- Heat the tensile specimen to the heat treatment solution temperature and hold at this temperature for 20 minutes.

- Cool the tensile specimen at a specified cooling rate (representative of the cooling rate during the actual quenching process) from the solution temperature to the test temperature, then hold at the test temperature for about 10 minutes for temperature stabilization.

- Conduct tensile testing at this test temperature at a strain rate of 0.005 in/in/minute to yield, then at a strain rate of 0.05 in/in/minute to fracture.

- This thermal cycling procedure follows the thermal history of the forging during heat treatment and so the data generated is representative of the heat treated material.

- Conduct the tests over the temperature range from RT to the heat treat temperature.

- These tests give both the Young's modulus and the plastic behavior of the material.

3.3 Stress Relaxation/Creep Tests

There are two methods for generating the data needed for modeling the stress relaxation behavior during aging. One is to use stress relaxation curves for the appropriate temperatures and heat treatment condition of the aging cycle. The second is to use data from creep tests. The stress relaxation test consists of pre-straining a tensile specimen to a high elastic strain, or just over the yield limit. The displacement is then fixed and the stress relaxation curve is recorded for the entire aging time, if possible. Typically for superalloys, stress decreases linearly with log(time). In a creep test, the strain is measured under a given applied stress which is held fixed over time. The stress relaxation technique require fewer tests than the traditional creep technique to cover the entire stress/temperature/time behavior of the material. Stress relaxation curves can be converted to creep strain rate versus stress for use in finite element models to analyze stress relaxation. It is critical to generate this data with the appropriate microstructure material.

3.4 Thermo-Physical Property Tests

There are ASTM standard tests for measuring the various thermo-physical properties: thermal expansion coefficient, thermal conductivity and heat capacity and so these tests will not be described here (see article on Thermophysical properties in this Handbook).

3.5 Heat Treat Thermo-Couple Tests

Heat transfer coefficient (HTC) data should include transfer from the furnace to the cooling station in addition to the main quench itself (fan, water, polymer, salt or oil). Typically the heat transfer coefficients are a function of temperature and the position on the workpiece. These data are specific to the quench facility used. Accurate heat transfer coefficient data are critical for correctly predicting residual stresses and subsequent machining distortions. The prevalent method of determining HTC's for furnace heatup, transfer and quench (various media) uses thermal data from a quenching experiment (Figure 12). This method involves a number of subjective decisions that can significantly impact the accuracy of the results. Inverse methods (2-D or 3-D) for obtaining HTC's are prone to instability and non-unique solutions. Problems exist on the validity of transferring a set of HTC's obtained on one shape to a different shape and in capturing localized distributions at critical geometrical features. An alternative method is to use computational fluid dynamics (CFD) to predict coolant flow and obtain HTC's using well-established correlations to fluid flow. CFD has only been used occasionally for this purpose due to its complexity and lack of accuracy for boiling heat transfer in oil or water quench.

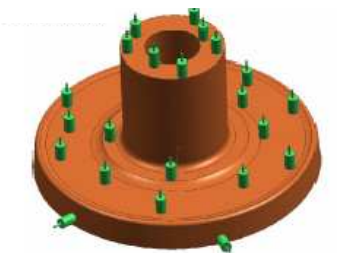

Figure 12. Heat transfer coefficient measurement using a thermo-coupled disk.

3.6 High Strain Rate Flow Stress for Machining

For realistic modeling of the machining process, accurate material property data are needed. Flow stress data are needed over the range of strain, strain rate and temperature that exist in machining operations. Obtaining the flow stress for use in metal cutting simulation is difficult because of the high values of strain and strain rate that are involved. Conventional tests (e.g., compression and tensile tests) cannot be used to obtain reliable flow stress data under cutting conditions. Flow stress data were measured for mill annealed Ti-6Al-4V and for alloy 718 by the Engineering Research Center for Net Shape Manufacturing (ERC/NSM) at The Ohio State University. Cutting forces were measured for slot milling tests on plate samples. Flow stress was calculated from the experimental forces and plastic zone thicknesses. The flow stress data were then validated through FEM simulations of orthogonal turning. The advantages of this approach are reduced experimental effort and cost compared to conventional material testing (e.g. compression and tensile tests). Typical high strain rate flow stress data are shown in Figure 13.

This method is limited by Oxley's assumptions as follows:

- Tool edge is assumed to be sharp.
- Chip formation is of continuous type (no serrations).
- The width of cut must be more than 10 times the feed rate to satisfy the plane strain assumption.
- Stress and temperature on the shear plane and the tool-chip interface are averaged
- No built-up-edge appears on the tool.

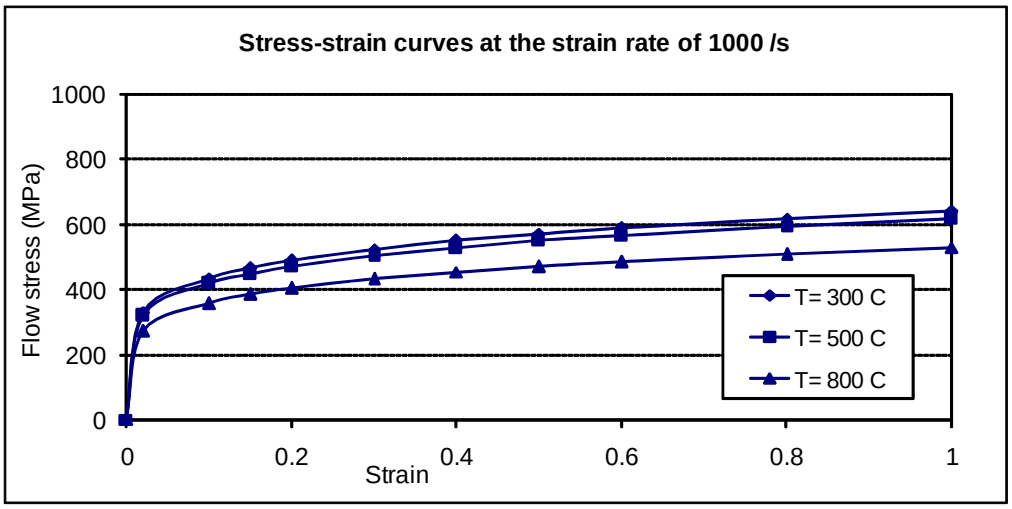

Figure 13. Typical high strain-rate flow stress data.

A methodology to obtain flow stress data suitable for machining simulation using inverse numerical analysis was developed. In the inverse calculation, the error between the measured cutting forces and the forces predicted by DEFORM™ are minimized using an optimization approach. DEFORM™ is capable of modeling the machining process in either a transient or a steady state mode. The steady state approach

is significantly faster (~15 minutes) than the transient approach (~20 hours) with year 2010 state of the art Personal Computers. The inverse analysis requires multiple simulations to reach the minimum of the objective function (least error between the measured and predicted cutting forces). To shorten the simulation time, the steady state approach was used to perform the inverse analysis. The 2D steady state method was validated by comparing it with the transient approach.

The Johnson-Cook flow stress equation was used:

$$\sigma_{\text{eq}} = (A + B\varepsilon^{n})\left(1 + C\,\ln\left(\frac{\dot{\varepsilon}}{\dot{\varepsilon}_0}\right)\right)\left(1 - \left(\frac{T - T_{\text{room}}}{T_{\text{m}} - T_{\text{room}}}\right)^{m}\right)$$

where σ_{eq} is the material flow stress; A, B, n, C, and m are five material constants; T is the absolute temperature; T_{room} is the room temperature; and T_m is the melting temperature.

The procedure was validated using experimental cutting force data from AMTC (Aerospace Manufacturing Technology Center). The process was longitudinal turning of a tube made of alloy 718. The inverse analysis was carried out on a Itanium machine, and it took about 31 hours and 70 iterations to find the minimum of the objective function.

4.0 RESIDUAL STRESS AND DISTORTION MEASUREMENT TECHNIQUES

4.1 Residual Stress Measurement

All residual stress measurement methods are indirect and rely on converting a measured strain (e.g., slotting, hole-drilling, ring-core) to a stress. The inverse procedure leads to high measurement scatter (>100% between different sources and methods) for complicated 3-D stress states. In addition, some destructive measurement techniques can change the residual stress state as part of the measurement itself. There is an ASTM standard which outlines the limitations of various measurement methods. Measurement techniques differ in respect of the stress components measured; depth (near-surface vs. through-thickness); mapping dimensionality (1-D, 2-D, 3-D); spatial resolution; sensitivity at low stress levels; destructive vs. non-destructive; and near-surface resolution. No single measurement technique is applicable in all cases and validation requires a combination of measurements depending on component geometry and surface vs. internal measurements. Validation requirements are dependant on the application requirements (manufacturing distortion, in-service distortion, lifing).

In x-ray diffraction (XRD) the stresses are obtained from the measurement of the crystal lattice strain. The stress obtained is an average over the x-ray beam volume. The accuracy of XRD depends on grain size and therefore, the material type. In order to measure the stress profiles inside or near the surface, some material has to be removed to expose the target area. This will affect the stress equilibrium in the component. Therefore, correction methods are needed to obtain the original stress before the material removal. In spite of these limitations, the measurement technique which is most robust for determining the machining stress profile is x-ray diffraction. However, even this method has the difficulty of collecting data at a sufficient number of points due to the small depth of machining induced stresses. Besides it is expensive to gather a large amount of x-ray data.

To test the applicability of the x-ray diffraction method in measuring machining induced residual stresses, measurements were performed on 4 specimens. Measurements were made at 0.0002” intervals up to 0.002” into the workpiece. Afterwards, measurements were made at 0.0005” intervals until 0.005”. Beyond 0.005”, measurements were taken at 0.001” intervals. These results were corrected for material removal at various depths. The x-ray diffraction measurements indicate high surface stresses, but with shallow depth. The stresses do not propagate greater than 0.001” below the surface (Figure 14). With

measurements taken at 0.0002" depth intervals, only 3 - 5 meaningful data points were obtained. The repeat measurement at another test laboratory indicated the same magnitude of stresses, but twice the depth of penetration. This shows the uncertainties and variability inherent in all stress measurement techniques. All measurement techniques are indirect and convert a measured strain to stress.

Other less common techniques can also be employed, such as micro-slitting, synchrotron, contour method, etc.

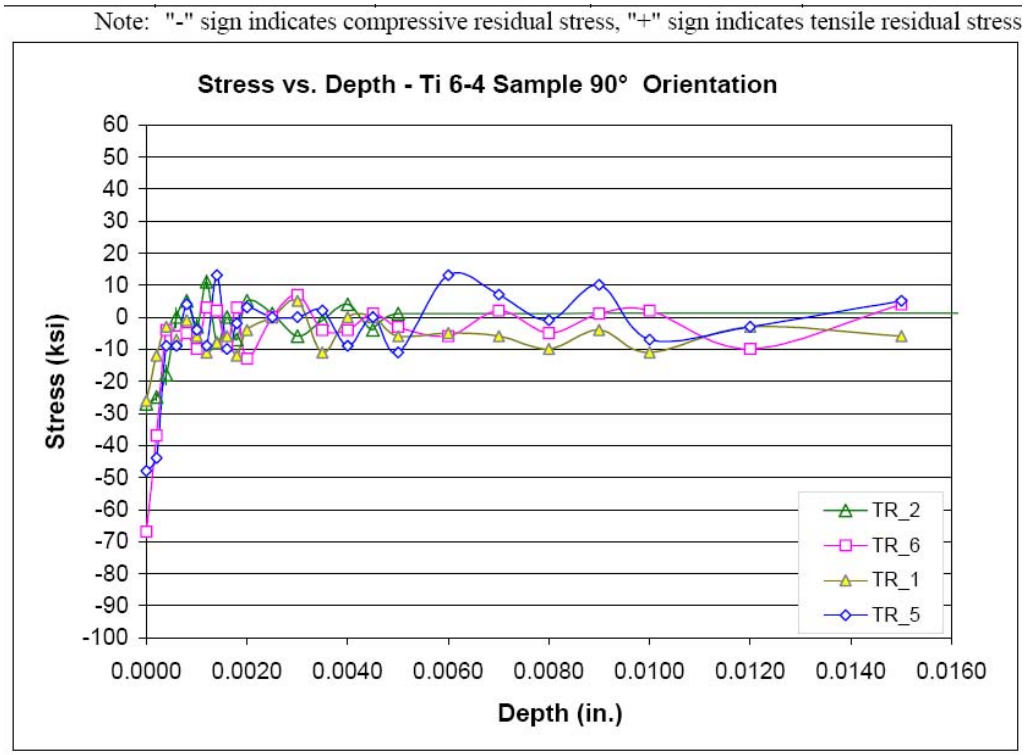

Figure 14. Residual stresses in the tool axis direction – XRD measurements.

4.2 Feasibility Demonstration of Micro-Slot Milling and Distortion Measurement

Tests were performed at Microlution, a designer and builder of micro-milling machines, to determine the feasibility of using micro-slot milling to remove very fine layers of material from the machined surface and measure the resulting distortion to investigate machining induced stresses present in the sample. Typically machining induced stresses are within the first few hundred microns from the surface in titanium. Figure 15 shows a schematic of this process. The sample is clamped near one edge, cantilevering the remainder. First, a measurement device (e.g., confocal laser) is used to measure the initial contour along the path shown by the dotted lines. Next, a small strip of material is removed by micro-milling in the form of a rectangular slot the full length of the sample with width w and depth d. The measurement along the dotted lines is then repeated to determine any distortion caused by the layer removal. This process is repeated multiple times to measure the change in distortion caused by each layer removal. The measured change in distortion is related to the removal of machining induced stresses present in the layer that was last removed and the stiffness properties of the sample.

For aluminum samples, the distortions are about 0.005" in magnitude. The measurement noise using a laser triangulation measurement systems is about 0.0001" - 0.0002". This provides a signal to noise ratio of 50:1 and the method is effective. However, the method was not feasible for titanium samples due to low signal to noise ratio at the surface where the larger stresses are located. The sample is stiffest during the removal of the first few layers, when nearly all of the material is intact, and most of the stresses are

present in the first few layers. Thus, the distortion measurement is least sensitive in the most critical regime.

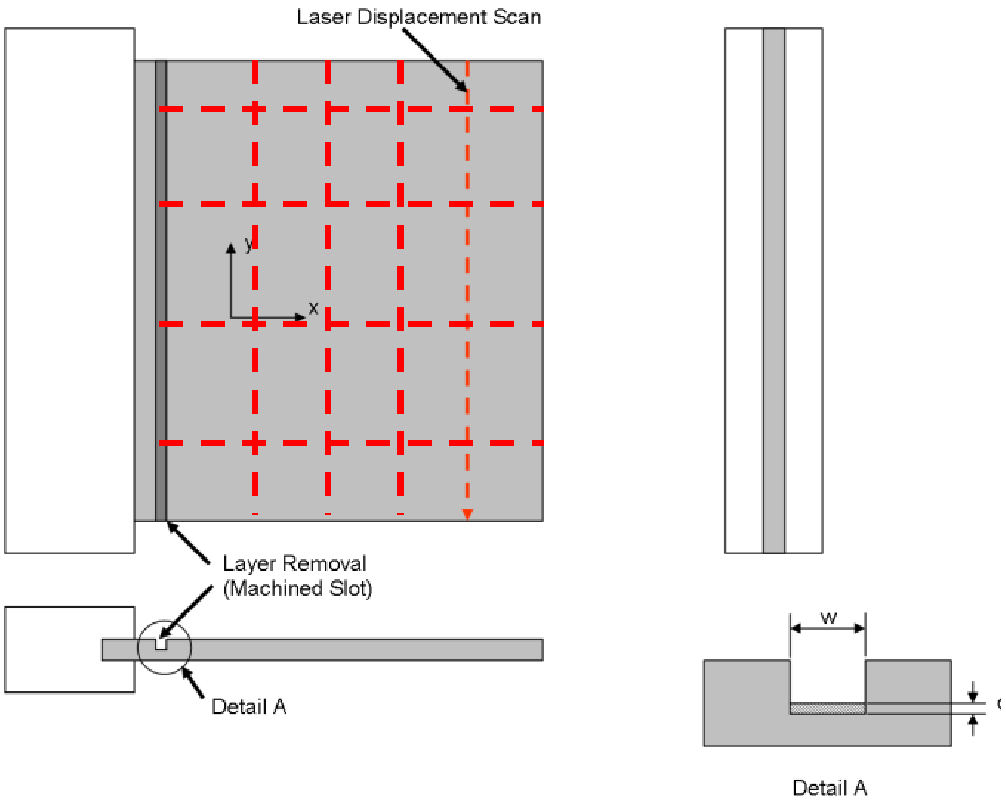

Figure 15. Layer removal and distortion measurement schematic.

4.3 Distortion Measurement

When validating the modeling predictions of machining distortions with experimental measurements, the data should be gathered on the face opposite to the one machined in the current operation, before and after this operation. The difference between the before/after measurements gives the distortion induced during this machining operation. This quantity should be compared with modeling predictions. Distinction should also be made between distortion when the component is clamped in the machine fixture versus the free-state when all external loads are removed.

If an attempt is made to correlate the modeling predictions of machining distortions with experimental measurements on a face just machined, this can potentially involve large errors. After the workpiece is removed from the fixtures, the free state dimensional inspection is made. The difference between the nominal undistorted shape and the free state dimension is the machining distortion induced during this operation. However, in practice, the nominal undistorted state may be slightly offset. Such offsets can occur since the workpiece is not perfectly flat or axi-symmetric and cannot be exactly positioned in the fixture on the cutting machine. So machining distortions induced during the current operation on the cut face are confounded with positioning errors. Axial drops on the just machined face measured relative to the reference point will be sensitive to the exact amount of material removed and the distortion which occurs as the material is being removed. Therefore, a realistic comparison of the predicted and measured distortions on the just machined face is difficult.

Dial indicators are the most commonly used for in-process measurement. When the component is still clamped in the fixture, one can use the machine turret to carry a dial indicator to scan the prismatic surfaces and note the distortion contour.

Coordinate Measurement Machines (CMM) are also very common for measuring multiple features on more complex parts (Figure 16). When compared with the modeling results, the model has to be in a free standing state unless the part stays in the same fixture during machining when presented to the CMM.

Optical scanning techniques (laser or fringe projection) have become more mature and more accurate in the recent years (Figure 16). It has an unique advantage because it is capable of providing a large amount of digital data of the component profile in a very short time which none of the other techniques can offer. Because of the size of the X/Y/Z point cloud data file (can be up to millions of data points), special software such as Geomagic, Polyworks, RapidForm, Surfacers, are needed to interrogate the data and compare with CAD models.

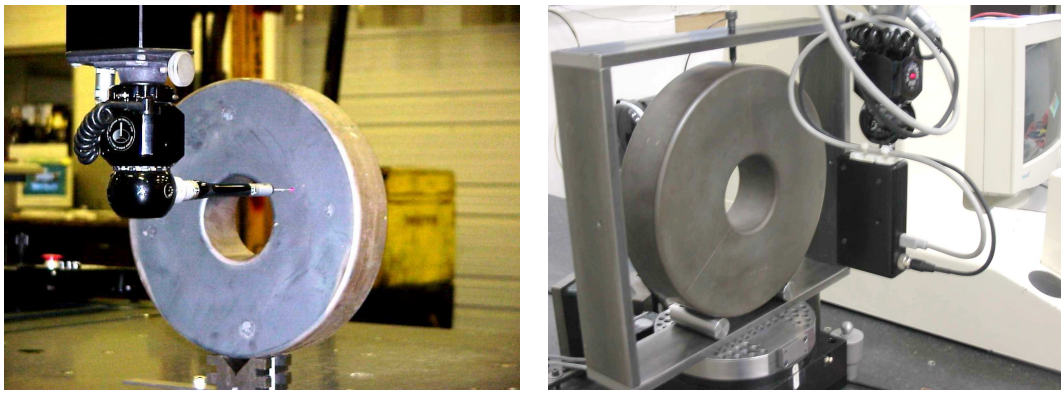

Figure 16. CMM inspection and optical scanning setup for measuring distortions.

5.0 MODEL VALIDATION ON ENGINE DISK TYPE COMPONENTS

5.1 2-D Residual Stress Validation on Engine Disk Type Components

Model validation was conducted first on simple pancake shapes and then on complex production shapes. The experimental heat treat conditions were selected to maximize residual stresses and subsequent machining distortions. The intent here was to intentionally generate large residual stresses and machining distortions in order to measure them accurately and avoid large errors in experimental measurements which can prevent meaningful model validation. The heat treat cycle consisted of heating the U720 forgings from room temperature up to the solution temperature of 2000^{o}F, holding at temperature for 2 hours, followed by a 30 second transfer time from the furnace to the fan cooling station, fan cooling for 10 minutes, after which the forgings were still air cooled back to room temperature.

The heat treatment of a production disk (Rolls-Royce AE1107/AE2100/AE3007 stage 2 turbine wheel, Figure 17) was performed for two cases: (a) the current oil quench process, and (b) a proposed fan quench process as a improvement of the current process. The current production oil quench process has high cooling rates. The proposed fan cooling process results in close to uniform cooling rate in a large volume of the forging of a magnitude which would meet the mechanical property requirements for the disk. This uniformity in cooling rate reduces residual stresses, heat treat distortions and subsequent machining distortions as compared to the highly non-uniform cooling rates achieved by the current oil quench process. The tensile residual stresses in the middle of the disk are reduced by more than 50% in the fan cool process as compared to the oil quench process. The heat treat distortion is reduced by about 70% in the fan cool process as compared to the oil quench process.


Figure 17. Machined Rolls-Royce production disks.

Residual stresses at the end of heat treatment were predicted. For simplicity, it was assumed that any residual stresses from prior forging operations were not significant and were relieved during the heatup and hold stage of solution heat treatment. This assumption is reasonable since the yield stress and creep strength of the material are small at the solution temperature and this would relax out any prior manufacturing residual stresses. The residual stresses in the forgings were primarily induced during quenching. Sensitivity studies were performed to establish that the results were only slightly affected (~5 %) with respect to finite element mesh size and variations in the heat transfer coefficients. An uncertainty of +/- 10% in the HTC's is typical of production conditions.

Given an accurate residual stress profile, well defined constraints imposed during machining, accurate material properties, and a well characterized metal removal plan, prediction of component distortion should agree reasonably well with measured dimensional changes. However, prior attempts to match measured distortion values against prediction have only shown qualitative agreement. The validation of complex models can easily be frustrated by experimental and analysis inaccuracies as well as by confounding of multiple effects. Therefore, a three-step statistically designed procedure was conducted which validates all the sub-modules and the overall model:

- Validate the thermal models by conducting thermo-couple tests.
- Validate residual stresses and distortions by conducting stress and CMM measurements.
- Validate machining distortions by conducting CMM measurements.

For each step, validation was done in a systematic step-wise manner by testing each feature in the model one at a time and then all together. This helped isolate the shortcomings of the model and rectify them before proceeding to an overall validation. Validation was performed on both simple and complex 2-D and later 3-D shapes, and on both airframe and engine materials.

Firstly, the thermal model was validated by conducting experiments using a pancake instrumented with thermo-couples to measure the thermal response during quench. Heat transfer coefficients were calculated from the measured temperature-time data. Good correlation was established between simulation and experiment, thus validating the thermal model. The same procedure was repeated on a production shape for both oil and fan quench. The accurate prediction of thermal response is a pre-requisite for the accurate prediction of residual stresses and subsequent machining distortions.

Radial and hoop residual stresses were measured along 3 sections and two clock positions (2 and 10 o'clock) in one pancake forging using x-ray diffraction. The measurements were conducted up to half the forging thickness. Selected stress measurements were repeated at another test laboratory to evaluate the reproducibility of the measurements and assess the accuracy of the data. The two sets of results differ by about 30 to 150%. The accurate measurement of stresses is difficult. Any stress measurement technique is indirect and relies on the measurement of a strain (either by strain gages, hole drilling, chemical milling, x-ray or neutron diffraction) and converting the strain to a stress measurement. This can lead to large errors in the measured stresses when the state of stress is tri-axial with a complicated distribution as

in these forgings. The large differences between the measurements from the two testing sources confirms the inaccuracies involved in the measurement of residual stresses. The validation of the model itself was based on measured distortion data.

Figure 18. Machining of slots during measurement of residual stresses.

A significant amount of material is being machined out as the residual stress measurements are made at increasing depth as shown in Figure 18. This material removal will influence the state of stress in the forging. The predicted residual stresses were corrected to account for the material removal. A 3-D 90-degree model of the forging was created and the two-dimensional residual stresses were mapped onto the 3-D model. In the 3-D model, the machining of the slots was carried out in depths of 0.3". At each depth, after the material was removed, the stresses and strains were allowed to re-equilibrate. This corrects for the state of stress due to material removal. The predicted stress after successive material removal passes was compared with measured values to provide a better assessment of the modeling predictions.

Figure 19 and Figure 20 show a comparison of the predicted and measured residual radial and hoop stresses at the three measurement positions. The measurements at the two o'clock and ten o'clock positions are compared with the 2-D predictions at the end of heat treatment and the 3-D predictions corrected for material removal. The 2-D predictions not corrected for material removal do not agree well with the measurements especially at increasing depth as more and more material is removed. On the other hand, there is good agreement between the measurements and the 3-D corrected predictions. The discrepancy between measurements and predictions is largest at the surface. Possible causes of this discrepancy are: residual surface hardening from machining not removed by etching; extrapolation of stresses from the finite element centroids to the surface; larger experimental errors near the surface where the stress gradients are steep. Repeat measurement(s) are shown by filled in dots and show the variability between two different measurement laboratories.

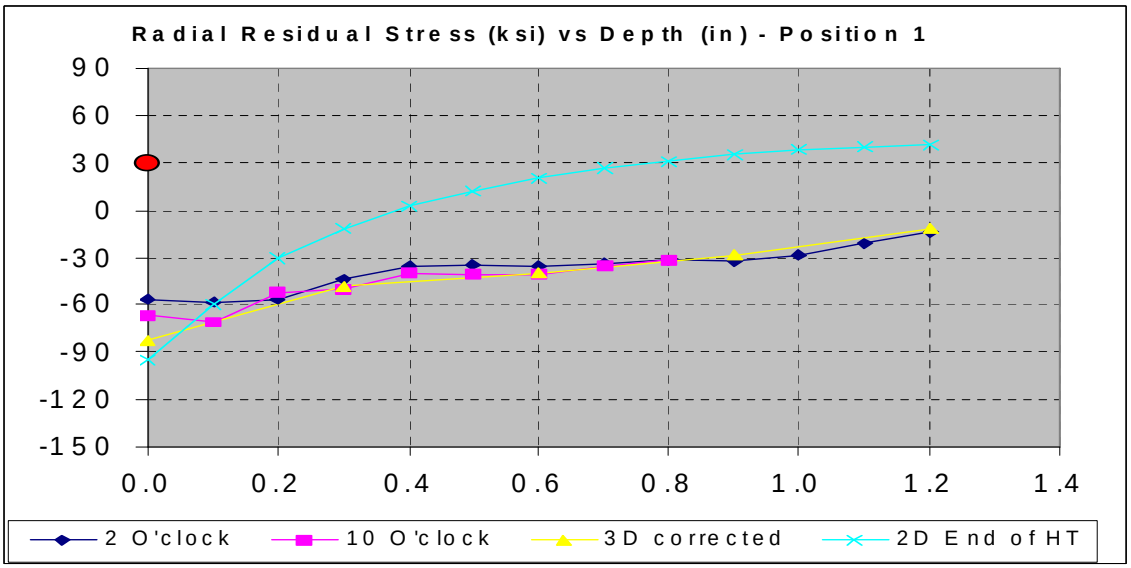

Figure 19. Comparison of predicted and measured residual radial stress.

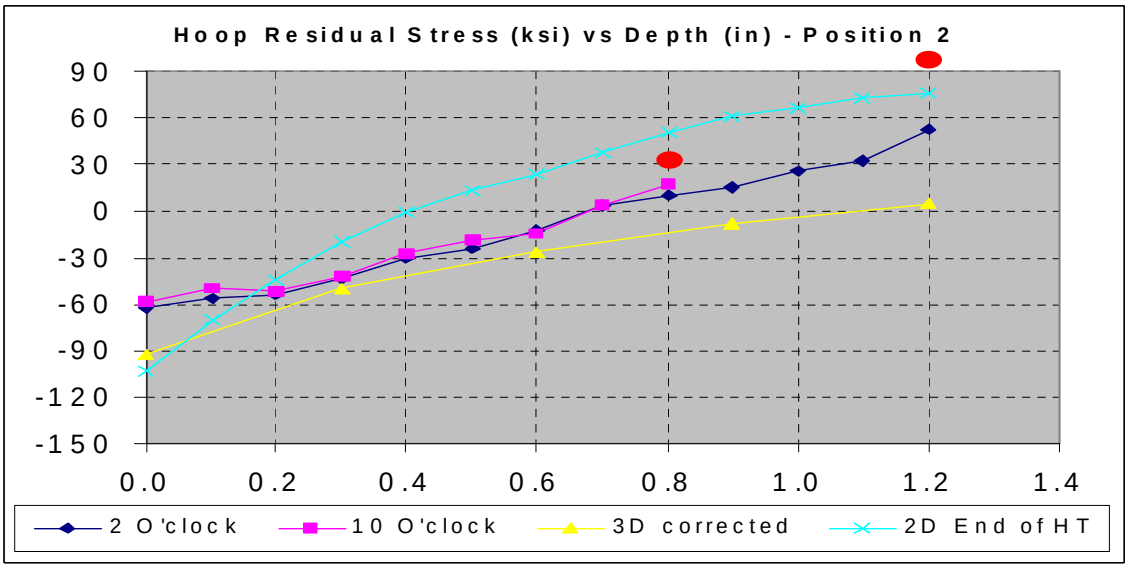

Figure 20. Comparison of predicted and measured residual hoop stress.

5.2 2-D Machining Distortion Validation on Engine Disk Type Components

Pre- and post-heat treat CMM inspection of the forgings consisted of taking measurements at various radial locations at 45-degree intervals to obtain the distortion induced during heat treatment (Figure 21). Forgings which were heat treated identically and which also had the same support during heat treat show similar distortions. This demonstrates that the measured heat treat distortions are reproducible. All the forgings had a 3-dimensional warpage as a result of the heat treat process. The measurements for the fan cooled forgings were more tightly bunched together showing less 3-D warpage with fan quench as compared with oil quench. The 3-D effect was averaged in order to allow a comparison with the 2-D cross section results which is based on the assumption that the component is perfectly axisymmetric (i.e., no warpage). The amount of non-axisymmetry decreases as the machining progresses. Note that the distortions are almost axisymmetric after machining. The non-axisymmetry introduced during heat treatment has been removed during machining.

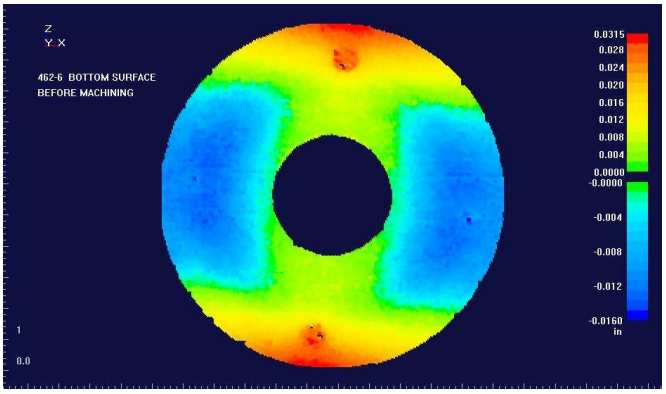

Figure 21. Optical scan data showing distortions after heat treatment.

The measured distortions are the result of deformations occurring during heat up from room temperature to the solution temperature, hold at solution temperature and subsequent quenching back to room temperature. The meaningful validation of predicted heat treat distortions is confounded by the interplay between several factors and by the fact that the distortions are small (~10 mils generally). The modeling predictions show the distortions induced only during the quenching part of the process. The measured and predicted heat treat distortions do not show good agreement since the distortions occurring due to creep and sagging during heatup and hold have been ignored in the model. The modeling of these distortions requires creep material property data at high temperatures and the inclusion of gravity induced sagging. This influences the distortions strongly. However, since the internal residual stresses are relieved during hold at solution temperature and regenerated during the cooling process, this assumption has a negligible effect on the prediction of residual stresses and subsequent machining distortions.

For the pancake forgings, the finished shape shown in Figure 22 was chosen for the purpose of achieving large distortion (for easy measurement). The material was removed in the four quadrants (top/bottom, ID/OD). Several alternate machining shapes were investigated, and this one chosen in order to obtain distortions in the 10 – 20 mil range. Distortions in this range are required in order to measure them accurately and avoid large errors in experimental measurements which can prevent meaningful model validation.

Figure 22. Forging after all four quadrants have been machined.

Initial predictions of machining distortions showed poor agreement with the measured data. For some cases, the predicted distortion was in a direction opposite to that measured. Measurements showed that the distortions caused by clamping forces while the forging was machined were negligible. All modeling inputs and procedures were examined carefully and five improvements were made to obtain better agreement between the measured and predicted residual stresses and machining distortions.

1. Exact stress-strain behavior instead of a simplified bilinear representation.
2. Strain rate dependency of stress-strain data.

3. Material removal in layers vs. "single-pass" – predicts right distortion direction.
4. Kinematic vs. Isotropic hardening.
5. Temperature dependent Poisson's ratio.

Of these five changes the first three had the most significant effect on modeling predictions. The last two had a smaller effect. The plots shown here (Figure 23 - Figure 25) are a small sample of all the results and show the general behavior. These figures show in general a good agreement between the predicted and measured machining distortions, considering the extent of non-axisymmetric deformation at some operations. In most of the cases, the agreement is within +/- 20%. When the distortions are very small (< 5 mils), the noise in the measurements is large relative to the measurement. This can show up as a large percent error but small absolute error. Process improvements by changing the machining sequence have been demonstrated using the model and were implemented successfully resulting in cost savings.

The conclusions of the distortion validation study are:

- Distortion measurements are more reliable and were used for model validation.
- Measurements and predictions show the same trend for all cases.
- Predictions agree better with measurements for smaller depths of cut.
- Predictions agree better with measurements for oil quench than for fan quench.
- Moving the finished shape axially changes the distortion about the same as the 3-D variation.
- The machining distortions are ~50% with fan quench than with oil quench due to reduced residual stresses. This is a potential process improvement.
- Possible reasons for discrepancy:
  - 3-D heat transfer coefficient variation not exactly captured in the 2-D axisymmetric model.
  - Inaccuracy in extrapolated low strain rate stress-strain data.
  - Sag in the furnace: effect of heat treat fixtures.

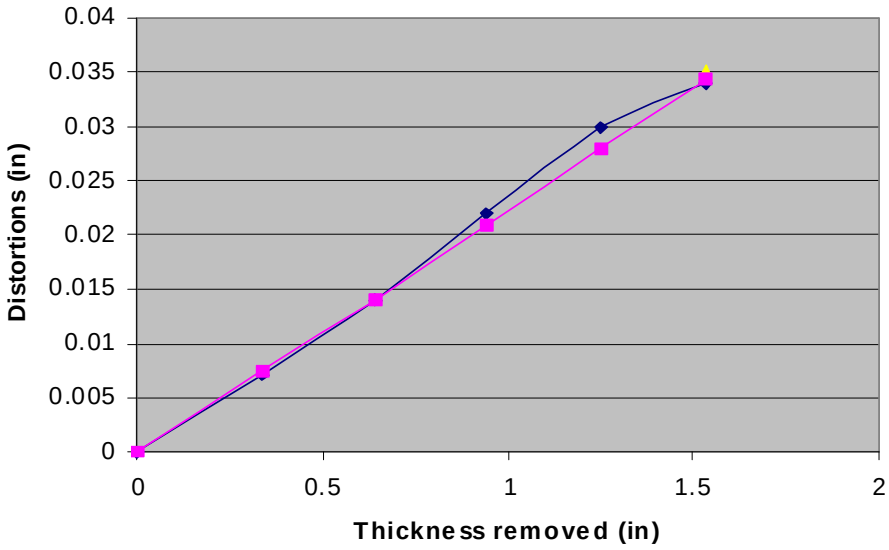

Figure 23. Comparison of measured and predicted distortions for pancake forgings.

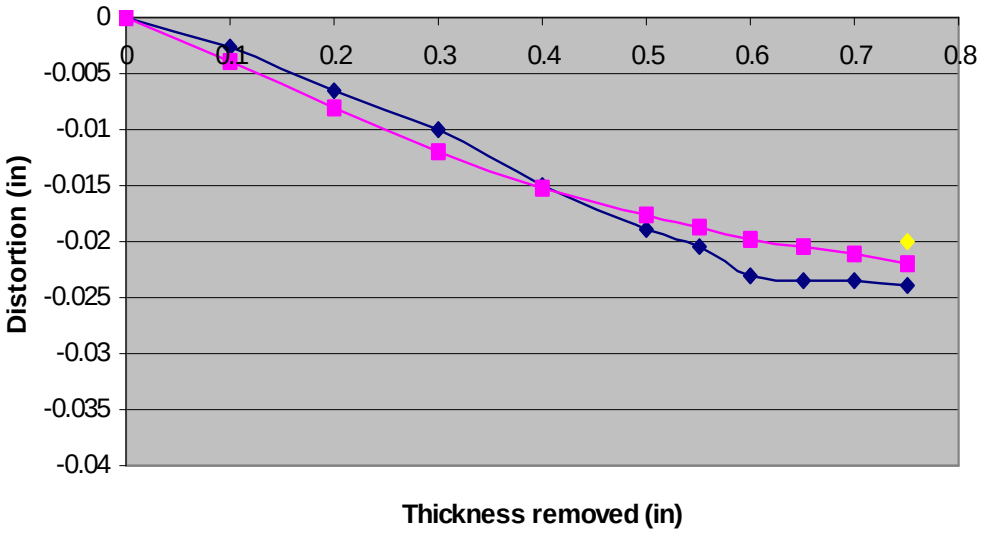

Figure 24. Comparison of measured and predicted distortions for pancake forgings.

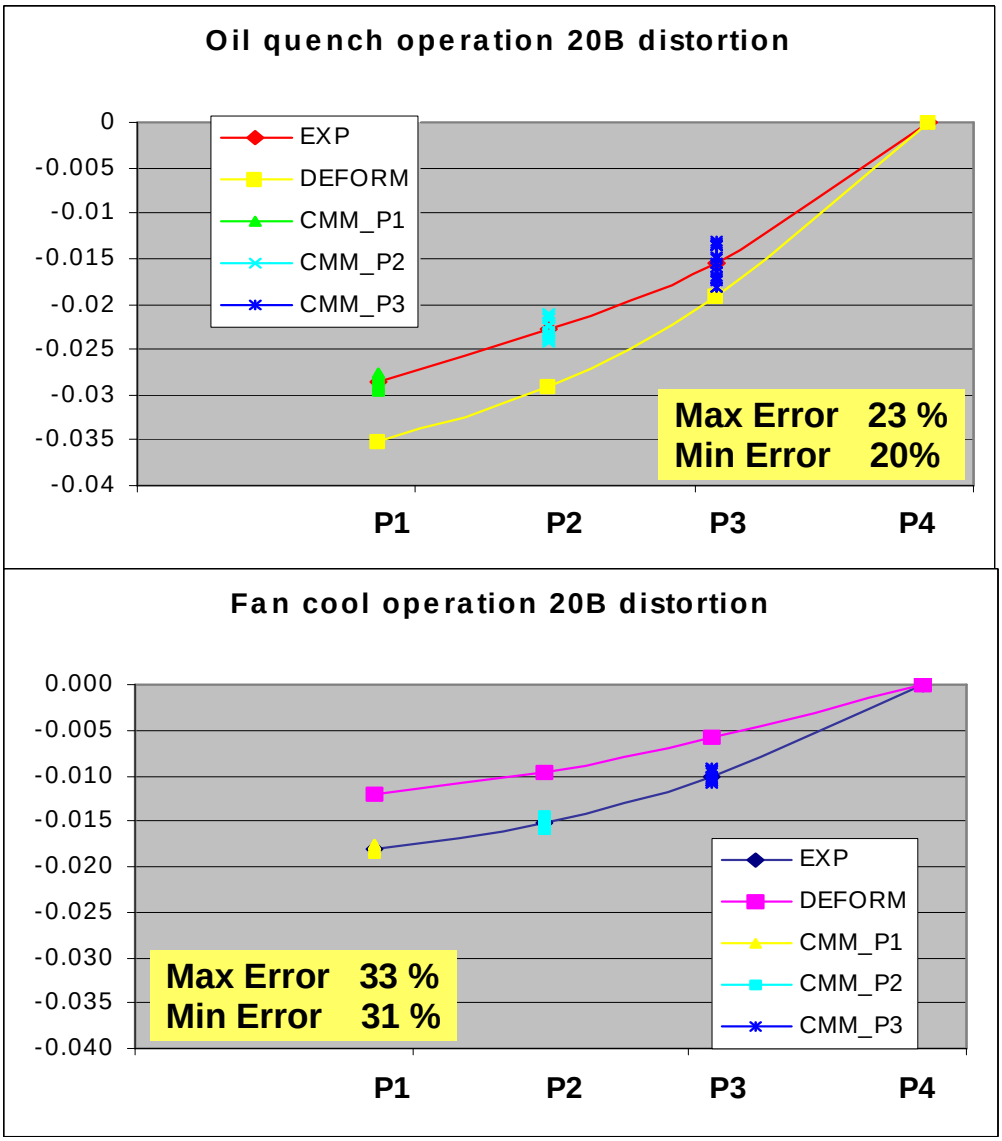

Figure 25. Machining distortions: fan vs oil quench. Distortion data represent the average of the eight experimental measurements at 45-degree intervals; the data points (CMM) show all the eight measurements and the extent of non-axisymmetric distortion; DEFORM™ represents the modeling predictions.

In practice, material is removed on one side of the component, the component is flipped over, and material is next removed on the other side. This process is repeated until one gradually approaches the finished component shape by successively removing smaller amounts of material on each side. This needs a number of machining operations, especially for distortion-prone geometries and/or materials. A possible machining strategy is to model the material removal to increasing depths on one side up to the point where there is positive material left over the finished component shape. At this point, the forging would need to be flipped over and the process repeated on the other side.

5.3 2-D Machining Distortion Validation using NASA Data

NASA's IDPAT and AST programs studied residual stress and machining distortions in advanced disk alloys. This work was extended to predict the effect of heat treatment on residual stress and subsequent machining distortions of simple forgings made of the advanced disk alloy ME-209 [1, 2]. Four pancake shaped disks of ME-209, weighing approximately 100 pounds each, were isothermally forged to a pancake shape 14" diameter by 1.9" thick. The four forgings were given different heat treatments. Heat treatments 2, 3 and 4 produced a fine grain micro-structure as a result of sub-solvus solution temperature (2075^0F, 1135^oC), and were designed to yield progressively lower residual stress. The first heat treatment produced a coarse grained microstructure as a result of the super-solvus temperature (2160^0F, 1182^oC), and was included to provide a direct comparison with the sub-solvus, stabilized heat treatment. The dimensions of the four forgings were measured to obtain the initial distortion/warpage resulting from heat treatment.

DEFORM™ was used to simulate the four heat treatments, in order to predict the initial residual stress distribution prior to machining. Following this, two machining operations were performed (Figure 26) and consisted of two face cuts on the top surface of each forging. The first cut went to a depth of 0.24", and the second cut went an additional 0.24" for a total depth of 0.48". After each cut, the disk was unclamped and warpage and thickness measurements were made. These data were gathered under controlled conditions for multi-pass machining operations and are therefore, very suitable for model validation. Figure 27 show a comparison of the axial distortion data measured by NASA (dotted lines) and the simulation data from the DEFORM™ (solid lines) machining distortion model. The measurements show that the disks are not perfectly axisymmetric. The measured distortion are an average of the eight sampling points around the circumference. The agreement between measurements and predictions is very good. Similar good agreement was obtained for the distortion of the other disks also.

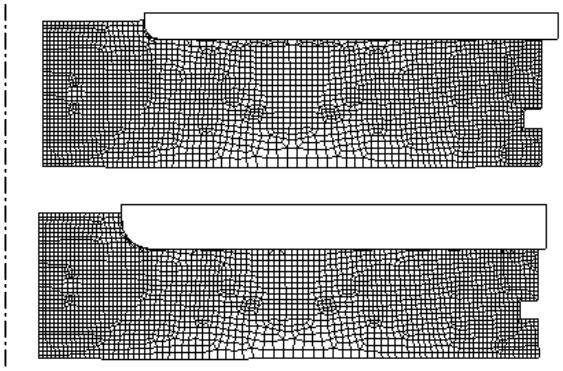

Figure 26. The two machining operations.

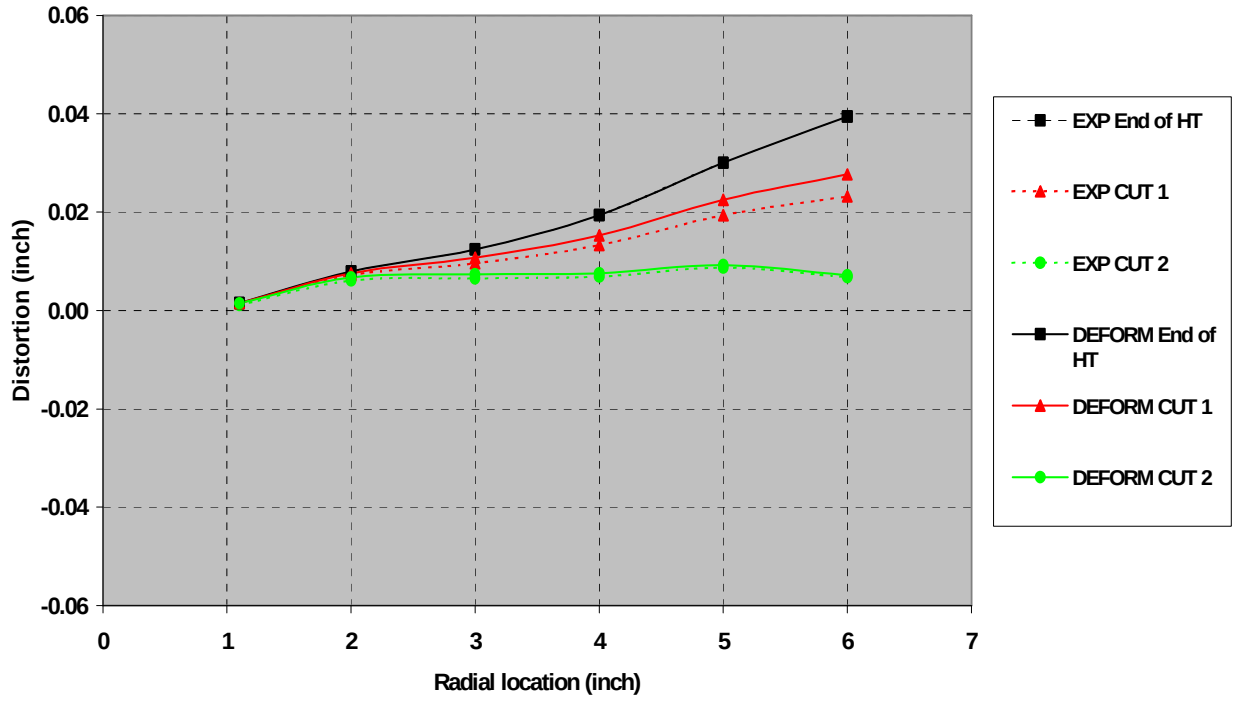

Figure 27. Good agreement between DEFORM™ predictions (solid lines) and NASA's measurements (dotted lines) of the axial distortions of Disk 1 after heat treatment and after two machining cuts.

5.4 3-D Model Validation on Engine Disk Type Components

The machined U720 forging shown in Figure 22 was selected for broaching distortion validation. The heat treatment and prior machining of this forging had been well characterized. Several simulations were carried out to define the machined geometry which would result in measurable distortions. Distortions should be large enough so that they can be measured accurately and used meaningfully for model validation. Small distortions are likely to have noise in the data making such data unsuitable for model validation.

Two slots, each 2" deep, were broached in the U720 disk (Figure 28). These slots simulate dovetail slots for blades in aircraft engine rotating disks. This was a well-controlled experiment to generate meaningful data for model validation. The finite element mesh was fine in the vicinity of the slot in order to accurately capture the stress and distortions in this region. Radial, axial, and hoop distortion measurements were taken in the slot region after the machining of each slot.

Two tapered pockets with a wall thickness of 0.2" were milled in another U720 forging (Figure 29). These pockets simulate features in airframe structural components. The pocket wall thickness was large enough to avoid distortions induced by cutting forces and surface residual stress effects. The finite element mesh was fine in the vicinity of the pockets in order to accurately capture the stress and distortions in this region. Radial, axial, and hoop distortion measurements were taken in the slot region after the machining of each pocket.

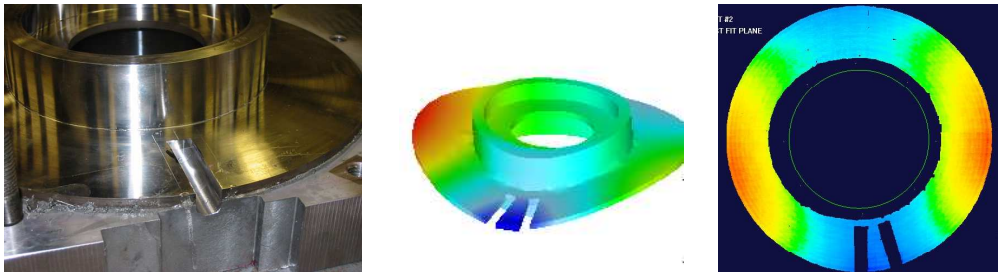

(a) U720 forging being machined (b) Predicted axial distortion (c) Measured distortion

Figure 28. Good agreement between predicted and measured distortions after slot broaching.

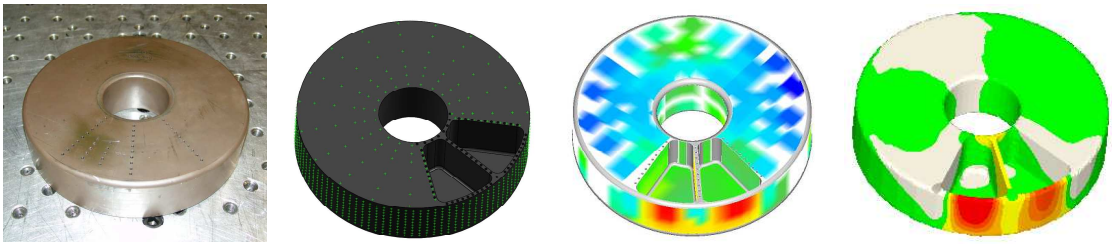

(a) U720 disk (b) Measurement Holes (c) Measured distortion (d) Predicted distortion

Figure 29. Good agreement between predicted and measured distortions after pocket milling.

Model validation was completed on experimental 3-D shaped components similar to production forgings. Alloy 718 pancake forgings were made from 8" billet, 120 lbs forged to ~14" diameter, 2-3" thick. One forging was used for gathering temperature data during quench for obtaining heat transfer coefficients. Figure 30 shows the comparison between measured and predicted temperatures at two thermocouples representing the best and worst matches. This figure also shows the layout of the thermocouples. A total of 13 thermocouples were used to capture the heat transfer coefficient variations around the forging.

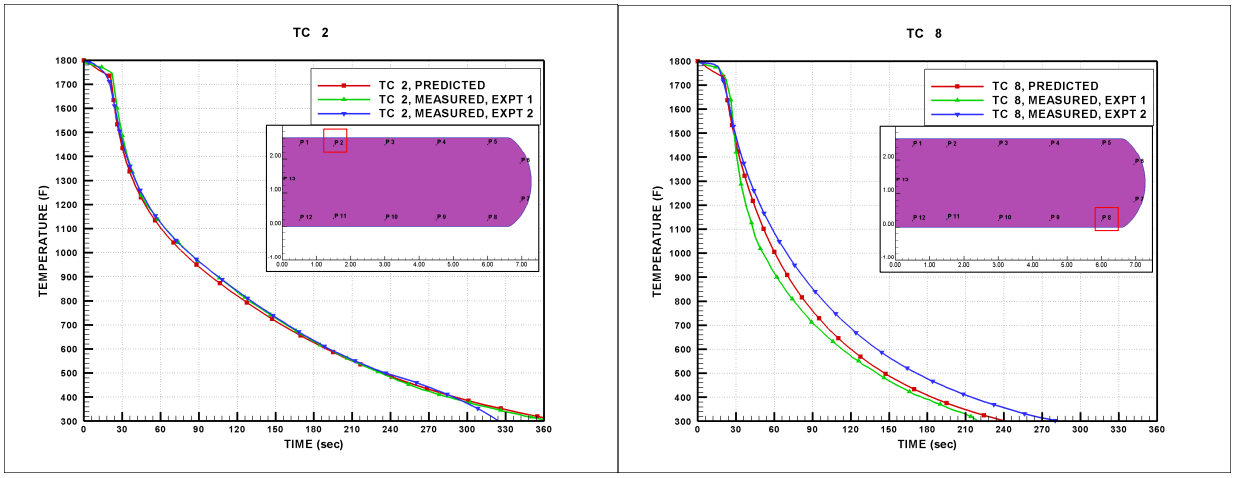

Figure 30. Comparison between measured and predicted temperature during water quench: TC's 2, 8.

Production disk like features were machined in four forgings, modified to accentuate the machining distortions: dovetail slots in the rim, holes in the web, and stem slots (Figure 31). Prior to machining the forgings, the process was modeled to define the machined geometry and machining sequence. The objective was to define conditions which would result in measurable distortions. Distortions were measured at each machining step. The measured distortions of each disk were compared to the

corresponding numerical prediction. A lot of data was gathered at all steps of machining. Here only the distortions introduced during the 3-D machining steps are shown for the four disks.

A comparison of the measured and predicted distortions at the stem (Disk 1) and at the OD (Disk 2) are shown in Figure 32. A comparison of the measured and predicted distortions at the OD (Disk 3) and at the stem (Disk 4) are shown in Figure 33. In all cases, the measured and predicted machining distortions matched within +/- 30% on average.

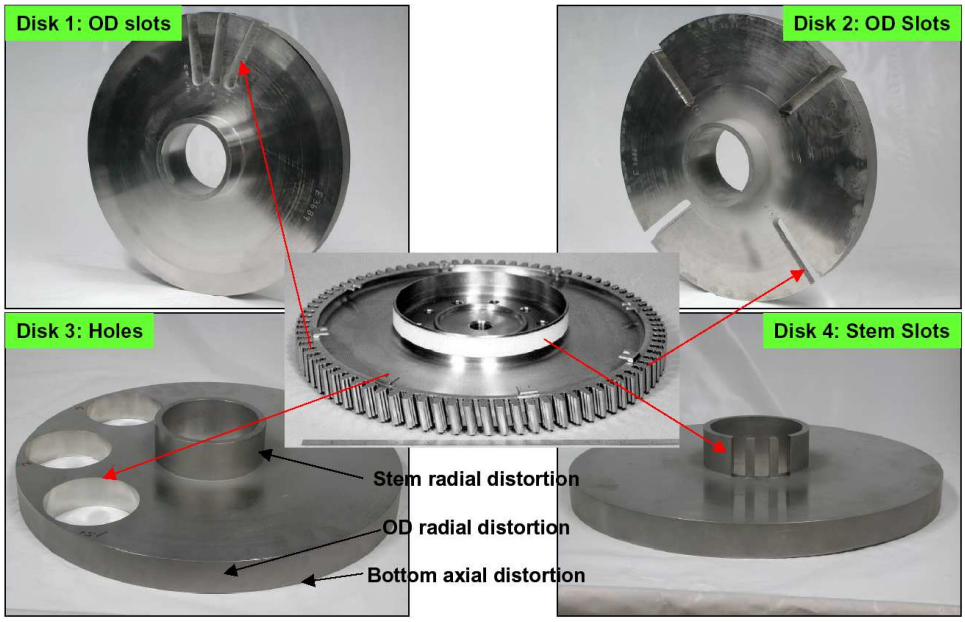

Figure 31. Machining of production like features in engine disk type forgings.

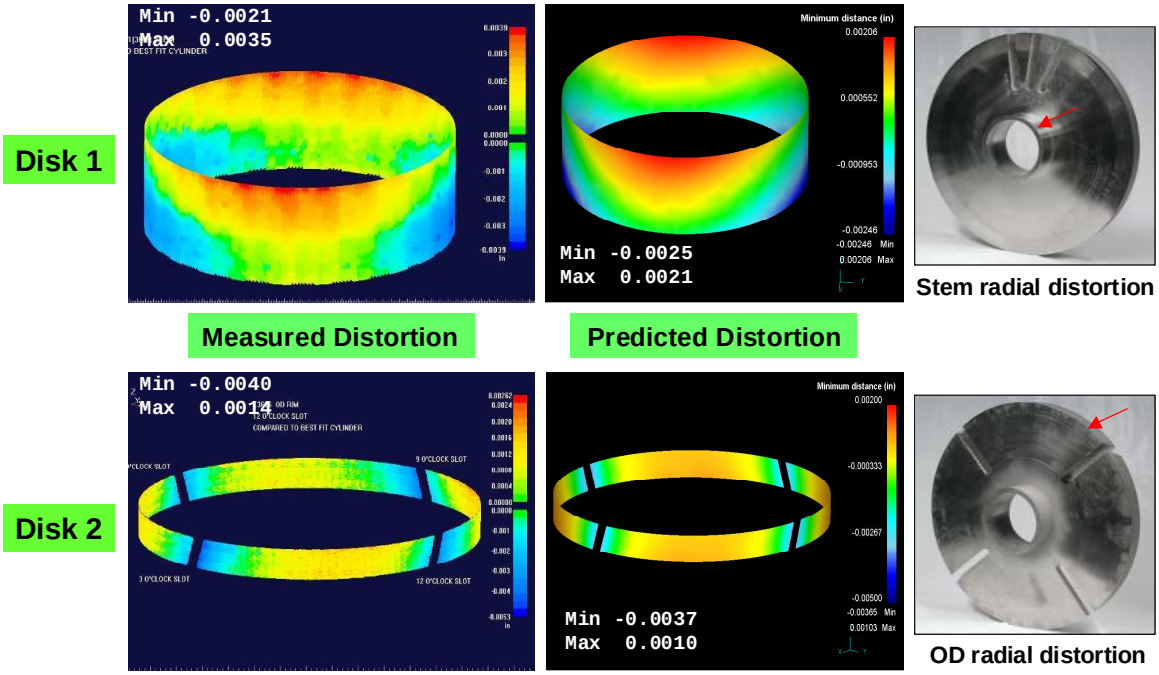

Figure 32. Comparison of measured and predicted distortions for disks #1 and #2.

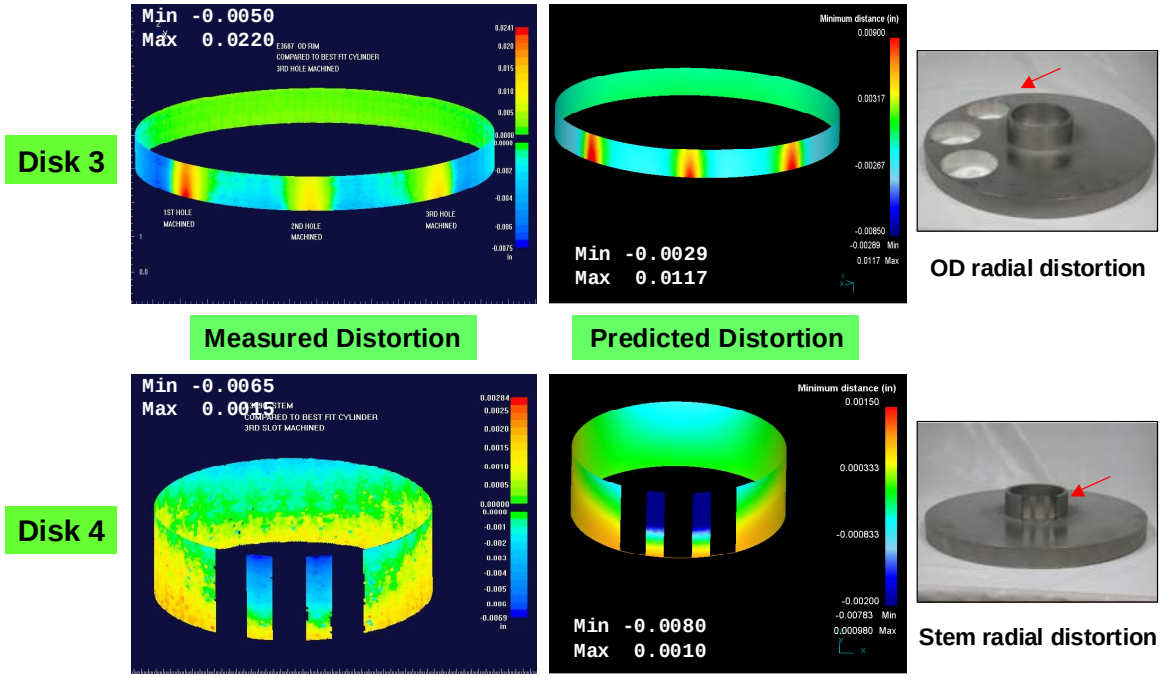

Figure 33. Comparison of measured and predicted distortions for disks #3 and #4.

Thermo-coupled trials, residual stress and machining distortion analyses have been completed on various production aircraft engine disks at the various OEM's. The modeling results were generally in good agreement with the measurements.

6.0 MACHINING INDUCED RESIDUAL STRESSES AND DISTORTIONS

For airframe type components, machining induced surface residual stresses are generally the main cause of distortions. The 3-D process model predicts component dimensional changes as a function of the initial residual stress state, the cutting tool forces, the machining induced surface stresses, the machining plan design, and the machine fixtures. Measurement and modeling of machining induced residual stresses and distortions in sub-scale rib/web geometries were performed. Machining induced residual stresses were obtained from one of four methods:

- Detailed finite element analysis of cutting process: slow, expensive to run, reasonable accuracy.
- Simple fast-acting mechanistic model: fast, cheap to run, reasonable accuracy after calibration.
- Semi-empirical linear stress model: fast, cheap to run, good accuracy after calibration.
- X-ray diffraction measurements: empirical, slow and expensive.

The first three are described in the following sections. X-ray diffraction measurements have already been described in the preceding sections. Stresses from these models and/or measurements were input into a 3-D distortion finite element model to predict component distortion. Distortion data was gathered after machining and compared with the modeling predictions.

6.1 Finite Element Prediction of Machining Induced Stress

Detailed finite element modeling of the machining process can be performed using commercial software like DEFORM™ or AdvantEdge (Third Wave Systems). Here results from AdvantEdge are reported. Simulations were performed using AdvantEdge for selected conditions of cutting speed, feed, radial and

axial depths of cut, cutter geometry (including edge preparation, axial and radial rake angles, number of flutes) and material grade. The simulations predict temperatures, forces and machining induced residual stress. The tool used had a 35 degree helix angle, 8-flutes, 19.05 mm diameter, with 3.048.mm corner radius and edge sharpness of 0.0508 mm.

Hole drilling measurements were conducted at Los Alamos National Labs (LANL). The error for each measurement was estimated as 5% by LANL based on historical evidence, with the exception of the first measurement (0.05 mm depth), which was estimated to have a 10% error due to the dish angle of the drill. Due to the nature of the hole drilling experiments, axial stresses could not be obtained and the first point measured was at 0.05 mm depth. Figure 34 shows a comparison of the predicted and measured tangential and the radial stresses for: cutting speed 121 smm, feed 0.0508 mm/tooth. Both exhibit maximum compressive stress values at about 0.05 mm, however the simulation results under-predict the magnitude compared to the measurements.

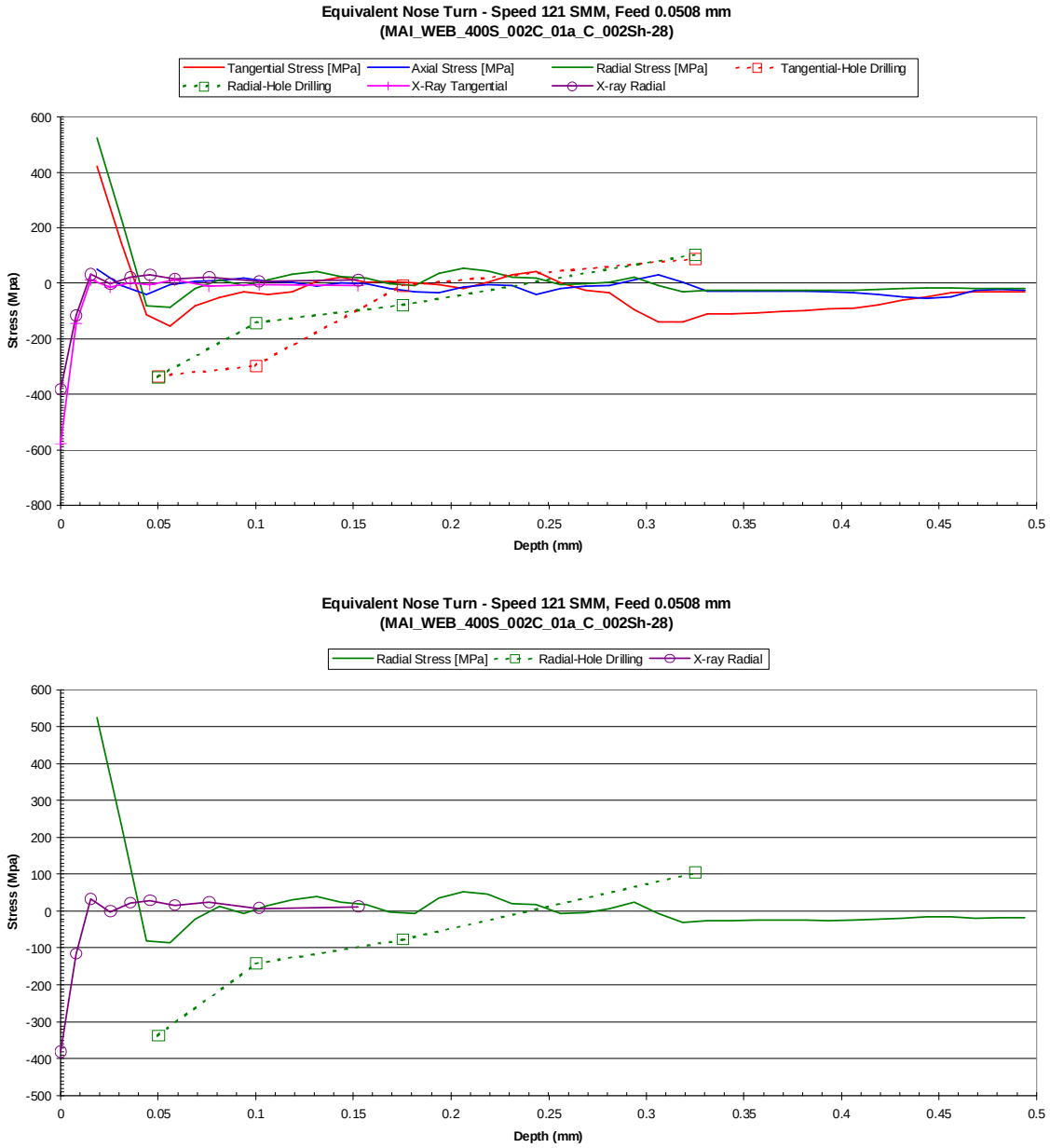

Figure 34: Turning/hole drilling comparison for: cutting speed 121 smm, feed 0.0508 mm/tooth.

AdvantEdge 3-D predictions satisfactorily captured the effects of variations in chip loads and cutting speeds on the workpiece residual stresses. Trends of peak stress as a function of feed and speed were similar between the simulations and hole drilling measurements. Cutting speeds were observed to have a significant effect on surface stresses in the simulations. With increased cutting speed (and correspondingly higher temperatures on the tool and workpiece), the surface residual stresses were observed to increase and become more tensile. Increased chip loads (feeds) were observed to have a pronounced effect on subsurface stresses. With increased chip loads, subsurface stresses (below peak compressive zone of stresses) were observed to become less compressive in nature. Mesh refinements did not result in a substantial change in the predicted results.

Detailed finite element models of the chip formation process are time consuming to run and are not yet fully validated. Meaningful results can be obtained if the cutting process can be approximated as 2-D (e.g., turning) with computational times of 4 – 8 hours. For 3-D cutting processes, several days of computational time is required. Therefore, these models are not yet production ready to be used in the industry on a routine basis.

6.2 Mechanistic Machining Model

Mechanistic machining models have been developed for quickly (in seconds as opposed to several hours or days for finite element methods) predicting cutting forces, temperature, and machining induced residual stresses for broaching and milling processes. The speed with which these models generate results provides the potential for analyzing a wide range of conditions in a short period of time in order to establish a set of conditions for use in a production environment. The overall procedure consists of obtaining cutting forces from the mechanics of cutting; computing stresses from the applied cutting loads; and relaxing the stresses to obtaining the residual stresses in the workpiece [3]. Mechanistic models need to be calibrated with experimental data and are good over a limited range of cutting conditions close to the calibration data set. The models predict the cutting forces reasonably well for both broaching and milling operations. The residual stresses are captured with respect to trends and depth of penetration. .

6.3 Linear Stress Model

Samples of ribs and webs which are representative of large airframe structural components were used to evaluate machining induced residual stresses and distortions. The principal stresses for rib coupons are aligned with the helix angle of the cutter. For the web coupons, the principal stresses are aligned tangential and normal to the cutter radius. Process parameters used as control variables included spindle speed, feed rate, cutting tool material, cutting tool geometry and edge sharpness which were defined using Taguchi methods. Ribs were made by finishing with the side of a cutter and webs were made with the bottom of a cutter. The geometry was chosen to allow a 2” x 2” sample for stress and distortion measurement. Industry standard milling cutters were selected to machine the samples (Figure 35).

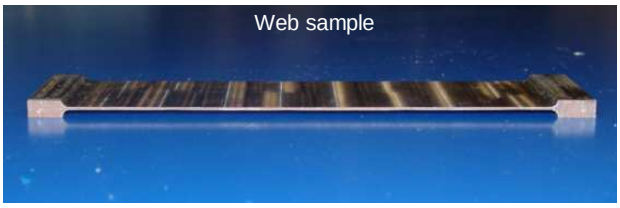

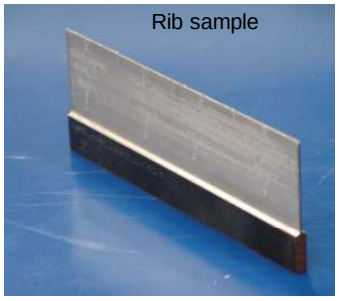

Figure 35. (a) Tungsten-Carbide and AISI-M-42 cutting tools; (b) Machining of subscale webs ; (b) Machining of subscale ribs.

A thin sample distorts after machining thus relieving some of the machining induced stresses. Therefore, the residual stress measured in a thin sample is *not* the same as the machining stresses. In order to accurately measure the machining induced stresses, samples much thicker than typical thicknesses were used. This eliminates the post machining distortion and partial relief of stresses and accurately captures the stresses induced by machining.

Based on the rib and web distortion experimental data, a linear stress model was developed for the mapping of residual stresses on an airframe type component and obtaining its distortion due to machining induced residual stresses. Based on experimental and numerical observations the following assumptions were made.

- Machining induced effects are concentrated in a thin surface layer.
- Machining induced effects from previous cuts are removed and a new surface stress layer is created during each pass of the tool. Therefore, only the machining parameters in the last pass are needed to determine the machining induced effects.
- Machining stresses depend on the thickness direction only and can be averaged over the machined surface.
- Machining induced plastic strains do not depend on the shape of the component for a given set of tools, material and machining parameters.
- Machining induced effects at joints (e.g., filleted regions) are not significant and therefore ignored for the determination of distortions and residual stresses.

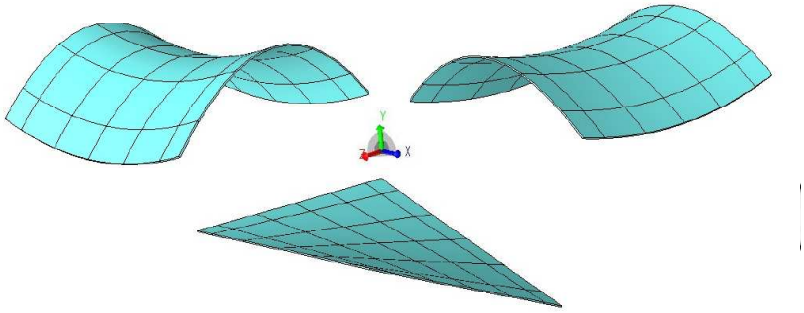

Figure 36. Displacement computed for linear shape functions: a) x-component, b) z-component, and c) xz-component.

The distortion of the rib and web samples was measured using laser interferometry. The measured distortion was fitted with polynomial functions (linear coefficients for the x-, z- and xz-directions). The three coefficients represent the bending in the two directions and the twist respectively. Figure 36 shows the contribution to the distortion caused by each one of the linear terms (x, z, and xz). The ability of obtaining a good fit of the distortion using linear terms indicates that the linearity assumption is valid. Coupons with a worse fit had small distortions with a small signal to noise ratio.

For a component which is a collection of ribs and webs of relatively uniform thickness joined by fillets, the distortion can be predicted by using as input linear terms determined through the experiments described here. Based on risk and cost and schedule feasibility, for production use, an empirical

combination of x-ray diffraction with calibration by linear stress modeling was selected. This approach combines the best measurement of the shape of the machining stress profile (x-ray) with the best measurement of the magnitude of the machining stress profile (linear stress model). The x-ray data defined the shape of the stress gradient as starting negative (compressive) and quickly decaying to zero. The coefficients in the linear stress model were obtained by matching the area under the stress profile (weighted by the distance normal to the surface). Figure 37 is one example of the stress input.

Four rib and four web coupons were modeled (Figure 38, Figure 39). The dimension of the rib and web coupons was 2 inches by 2 inches. The thickness of the coupon was assumed to be uniform. 8-noded linear brick elements were used. Surface meshes were generated to capture the initial stress variation through the thickness direction. Six nodal points are enough to capture this input curve. The coupon was then allowed to re-equilibrate under the applied stress field. The resulting distortion was compared with the measurements. Numerical tests were conducted to evaluate the effect of mesh size on the distortion results. Increasing the number of thickness layers had a minimal impact on the results. However, increasing the number of in-plane elements had a significant impact. A mesh size of 96 x 96 in-plane elements with 12 thickness layers provided a mesh independent converged solution.

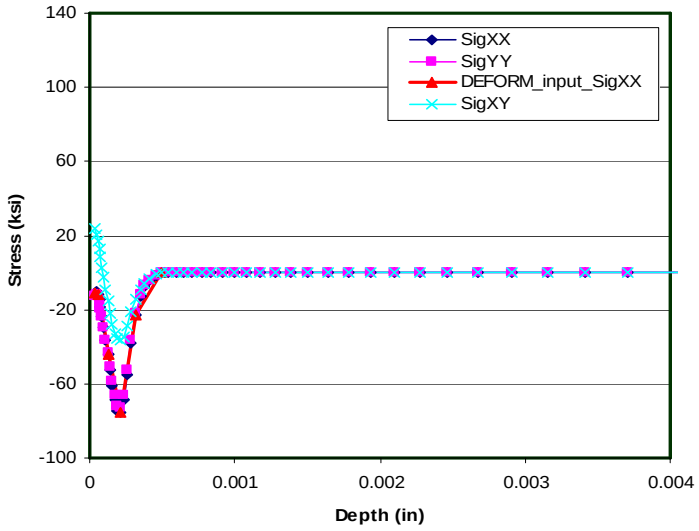

Figure 37. Example of stress input curve.

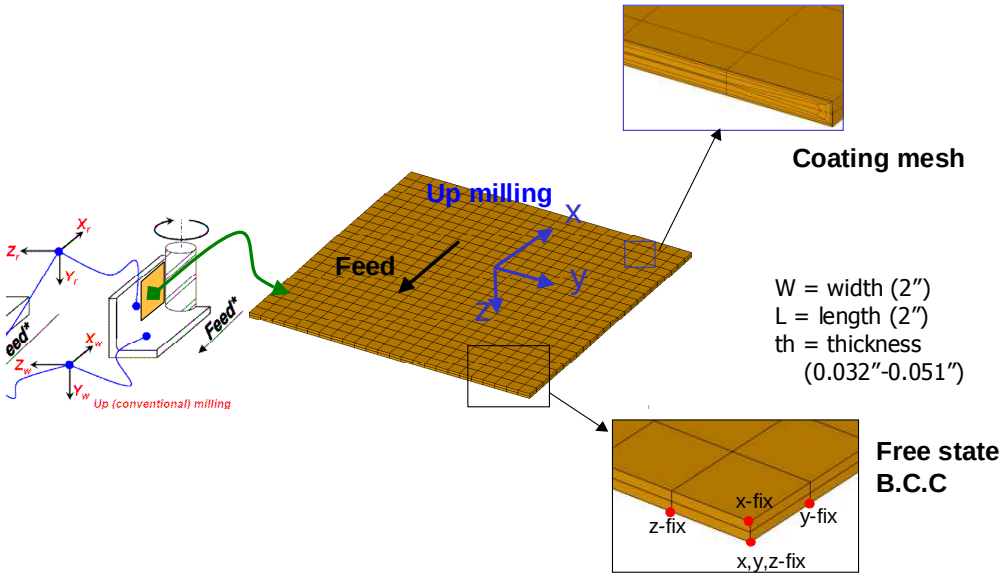

Figure 38. Finite element model for rib coupons.

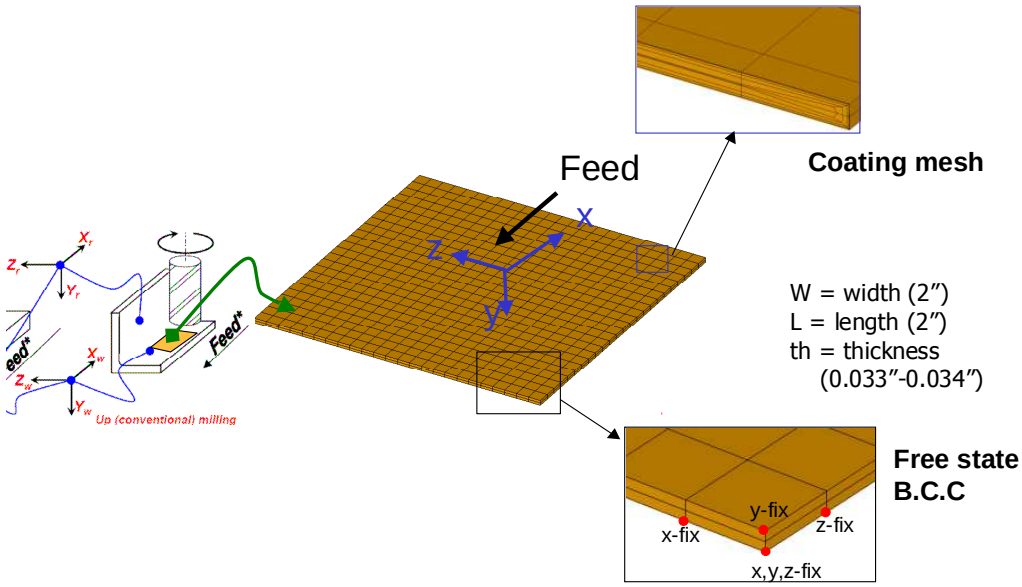

Figure 39. Finite element model for web coupons.

The model was validated on a selected subset of rib/web samples using residual stresses from a mechanistic model and from x-ray measurements. Figure 40 shows a comparison between the measured and prediction distortions for typical rib and web samples The ribs twist and the webs bow out which is consistent with prior experience. The error between the predictions and the measurements range from 2 to 29%. Similar agreement was obtained on production components which cannot be shown here due to proprietary reasons.

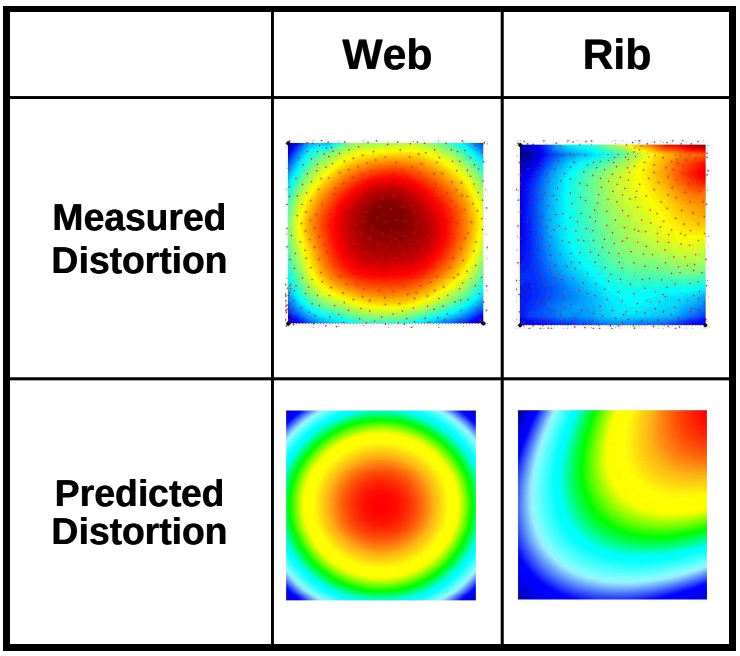

Figure 40. Rib/Web distortion: predictions and measurements match 2 – 29%.

6.4 Integration of Machining Stresses into DEFORM™

Inclusion of surface stresses and cutting tool forces is important for components with thin section sizes. Figure 41 shows a flow chart of the production distortion model. The machining stresses are imported into DEFORM™ using a graphical user interface taking into account the cutter direction, path, and type. The GUI enables easy error-free import of data. Bulk residual stresses, if significant, can be superposed on the machining stresses. The overall stress field is then equilibrated to obtain the component distortion. If the distortion is outside prescribed limits, the process is repeated with a different machining process until the distortions fall within the prescribed limits.

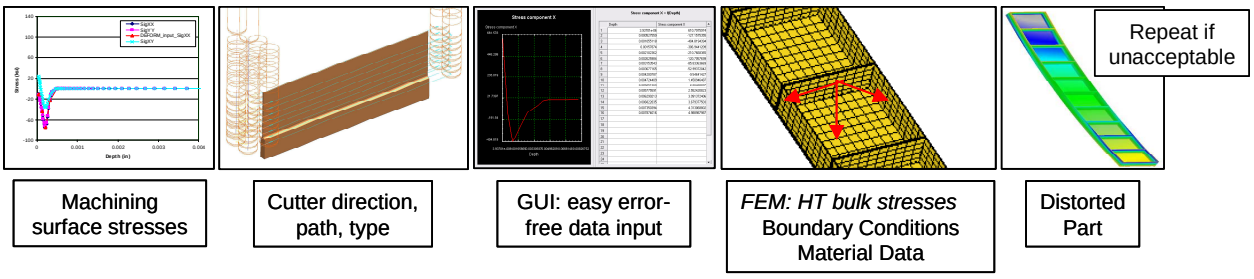

Figure 41. Production model flow chart.

The simulation procedure consists of these steps:

1. Generate a brick mesh for the final machined component.
2. Generate multiple layers of near surface mesh to capture the machining stresses.
3. Interpolate bulk residual stress from heat treatment to this mesh, if needed.
4. Import machining induced residual stresses to the near surface mesh (details below).
5. Carry out a stress equilibrium simulation.
6. Repeat the process for subsequent machining operations, if needed.

The following procedure was developed for importing cutting induced residual stress:

1. Generate a fine surface mesh.
2. Pick surface nodes in the region where the stresses are to be imported.
3. Input cutting direction for the region.
4. Define machining induced residual stress as a function of depth or a constant value.
5. Interpolate imported stress components to the mesh nodal locations. Rotate the stress components to the model coordinate system. The rib region is cut by the flutes on the cutter and the principal residual stresses in the cutting and the transverse directions are oriented with respect to the helix angle. The web region is cut by the bottom of the cutter and the principal residual stresses in the cutting and the transverse directions change depending upon the tool path direction.

Aircraft structural components typically consist of multiple thin walls as shown in Figure 42. In order to predict the distortion of thin ribs and/or webs, meshing of thin walls is important for accurate results. Since thin walls can be easily modeled by a structured mesh system, a brick mesh is often used for thin-walled aircraft components. The advantages of tet meshes are that it is possible to automate initial mesh generation, remeshing and near-surface mesh generation which makes it possible to automate the modeling of multiple machining operations. Since automatic brick mesh generators are not available, it is not possible to do this with brick meshes. However, brick meshes provide greater accuracy and a much smaller number of brick elements is needed to define large thin-walled airframe geometries which reduces the computing required. A large number of tet elements are required for thin-walled airframe geometries, thereby significantly increasing the computational effort. The selection of the approach will need to evaluated on a case-by-case basis depending on the component geometry, machining operations and the distortion information required from the model.

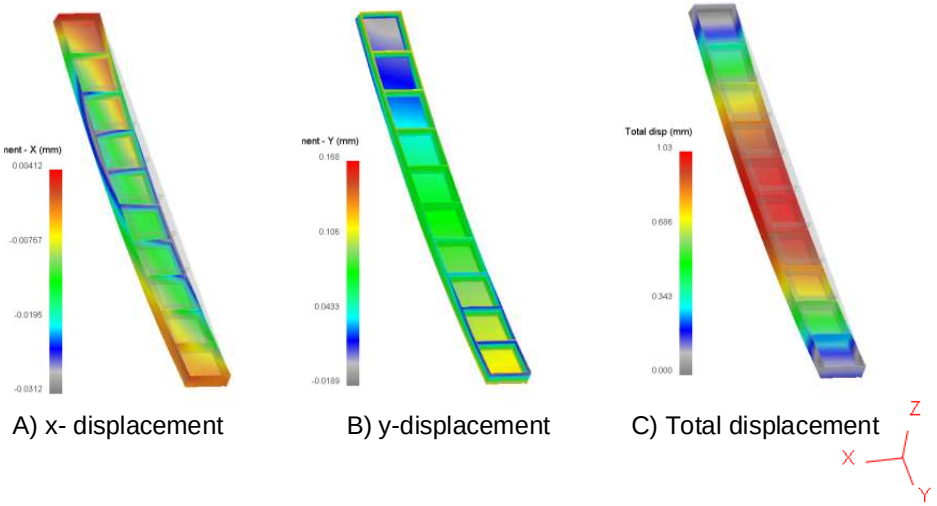

Figure 42. Machining distortion example.

Scientific Forming Technologies Corporation (SFTC) has developed a procedure to realistically model the machining process and streamline the analysis of multi-step machining with the commercially available software DEFORM^{TM}. A custom machining template was developed for a user to perform all the simulation steps in an automated sequence. A series of machining distortion simulations can be triggered from the procedure to simulate the complete process from the heat treat shape to the final machined shape. Due to the complexity with machining involving multiple passes and multiple operations, it is essential to graphically preview the relative location of the fixtures, workpiece, and machining paths prior to the analysis. This feature enables an up-front review of the entire material removal process and ensures that all data have been input correctly. .An important objective of the

improved machining simulation method is to bring the modeling analysis and methods into closer alignment with the physical machining process as understood by a machining process engineer. The key challenge is to achieve the appropriate balance between improved functionality and ease of use for the resulting simulation method.

Modeling steps include Boolean operation for material removal, stress re-equilibrium under clamping condition (after material is removed) and free state distortion (after clamps are removed). The approach starts with a residual stress pattern and distorted heat treat shape generated using DEFORM™ for heat treatment process modeling. These results are then mapped onto the mesh used for machining simulation along with the geometry of the machining plan generated using CAD software and NC machining information. The geometry, representing the machined shape, is then meshed, clamping loads are added, and machining is carried out through element removal. A subsequent analysis is required to verify that the tooling has sufficient stiffness to withstand the rebalanced loads following machining. The machined distorted shape is calculated following removal of clamping loads and the entire cycle is repeated for each operation of metal removal until the finished component shape is reached. The results are presented in a format that is directly comparable to dimensional measurements. Typical results are shown in Figure 42. For a realistic model size of a typical aircraft component, a total of about 150K elements are expected. Depending on the computer, solution method, and boundary conditions used, this model has a run time of about 15 minutes to 3 hours. Therefore, it is concluded that using DEFORM™ with the brick approach can be practical from the perspective of computational requirements.

7.0 MODELING BENEFITS

Although machining is a mature manufacturing process, the drive toward affordability continues to press established machining operations to increase metal removal rates, increase machine utilization, and eliminate machining steps. These efforts are worthwhile because machining costs are a very significant fraction of the total cost of manufacturing for aerospace forged components.

In the near-term, savings will be due to: reduced machining costs, reduced scrap, improved manufacturing lead and cycle times, reduced time to first article, and improved component performance and life during service resulting in reduced operating costs. A more significant additional cost savings is the ability to go to nearer-net-shape forgings after this technology has been more extensively validated. Accurate prediction of distortions will enable a reduction of the material envelope needed to compensate for distortions especially for the high-cost powder metal alloys used in rotating disks. The technology developed here is applicable to all military (USAF and USN) and commercial aircraft and engines.

The program is well aligned with the philosophy to achieve affordable metallic materials and processes with accelerated implementation for aerospace systems. Benefits are a reduction in acquisition costs of metallic components. Additional benefits also include potential for design of more robust components which have reduced tendency to distort during engine operation which may affect engine clearances and efficiency and engine performance.

Modeling provides a data-driven understanding of residual stress, validated commercially supported tools, and standardized modeling and measurement procedures. The MAI Programs represents a major technology advance for the industry and have advanced the state-of-the-art to a user-friendly, validated, commercially supported, and production ready analysis tool for 3-D machining problems, which can be used to achieve significant cost savings. Since process modeling can be used to improve both the fabrication processes and the component performance during service, it should be incorporated into the integrated design environment in the organization to achieve Design for Manufacturability and Design for Process Excellence. Various design disciplines can take the advantage of process models, such as; lifing, inspection, supplier-OEM collaborations, repair and overhaul.

The supply chain consisting of manufacturers of aerospace components, in addition to the OEM's, stand to benefit from the use of modeling. The OEM's will see a reduction in machining costs and the forging suppliers will benefit by being able to better control the heat treatment process. Distortion problems pose the biggest challenge on new components and/or new suppliers. Modeling technology will help shorten that learning curve. Current components with distortion problems will benefit during change of suppliers. New components will benefit right from the start. Although modeling has been demonstrated here for only selected engine and airframe materials, the model/method is pervasive and can be applied to other materials adding to the total savings.

The methodology of this program will include the capability to evaluate the full range of process conditions for production hardware and define process sensitivities relative to material and process variations early in the production process. This information will better define the process window. In addition, these tools could be used for evaluations once it was determined that the process window was breached.

8.0 MODELING IMPLEMENTATION IN A PRODUCTION ENVIRONMENT

Successful completion of the various MAI programs has permitted the technology implementation on a wide variety of components. Implementation has occurred initially on new components in which process(es) could be integrated into the original design, thus reducing or eliminating additional certification costs. Subsequent production implementation to address distortion problems on existing components is based on the cost benefit balanced against any additional certification costs. Specific applications with noted cost-reduction potential include: superalloy rotating components and titanium structural components. Implementation of the 2-D model is more wide-spread and it has been used for several production components successfully at several OEM's. As the models get more accurate with more validation, use and benefits will grow.

The mode and extent of use of the machining model will be somewhat user-specific depending on the extent of validation carried out, the problem the user is trying to solve or avoid, the certainty with which the various boundary conditions and material property data during heat treatment and machining can be quantified, etc. Here only some general guidelines can be provided. The general implementation approach is shown in Figure 43. The details of implementation will differ for large/small suppliers and airframe/engine components. OEM's, forge/heat treat suppliers, and machining suppliers are involved at various stages.

This work demonstrates that finite-element modeling can be a powerful tool to predict the residual stresses developed during heat-treatment processes and the distortion during machining operations. The use of commercially available software minimizes maintenance and enhancement risks. The machining template in DEFORM™ also provides an easy way to model the distortions developed during multi-operation machining sequences. These models have been integrated with standard engineering tools and implemented within the modeling organizations at the OEM's and at their forging and/or machining suppliers.

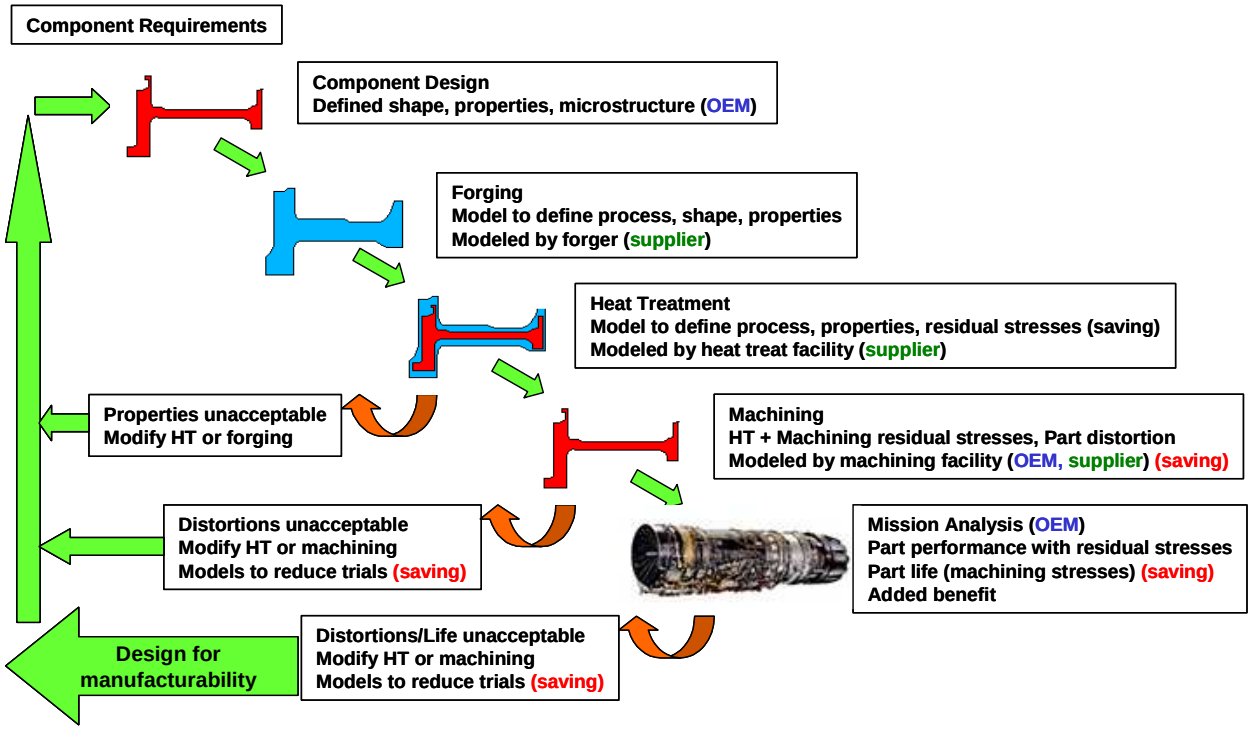

Figure 43. General implementation approach.

9.0 FUTURE WORK

Future work should focus on establishing standard material characterization, measurement and modeling methods to ensure accurate and repeatable residual stress predictions. Additional model validation on more materials and different types of components is also needed. The following paragraphs describe in detail suggested future work.

Roadmap: A road-map is needed to formalize plans to address the various issues relative to residual stress modeling, development and rapid implementation of modeling tools that link various materials and process models and provide a known level of accuracy and uncertainty. The roadmap should identify risks and a risk mitigation plan, balancing risk, cost, payoff, and maturity. Lessons learned from engine programs should be leveraged to airframe components recognizing the tremendous scale up in computational requirements from 2-D engine disks to large 3-D airframe components.

Modeling and measurement accuracy: In order for the modeling results to be useful, different levels of accuracy are needed depending on the application. The bulk residual stress modeling and measurement accuracy required for a range of applications should be established, including manufacturing (heat treat and machining distortions), service (dimensional stability), lifing (fatigue life, crack initiation and propagation), and material characterization. Various residual stress measurement methods should be compared to develop standardized procedures and recommendations. An assessment of the accuracy and variability of the predicted and measured residual stress profiles and its impact on manufacturing, service and lifing should be determined. Model accuracy, capability and user-friendliness should be addressed to obtain an industrially usable tool.

Material data: Material constitutive properties (tensile and creep) are needed as inputs to the residual stress models. Development of standard material test methods (on-cooling tensile and creep/stress relaxation) and an industry-wide data set for commonly used alloys will reduce uncertainty and improve modeling accuracy. These data sets could more thoroughly cover the full range of temperatures, strain rates, and microstructural conditions than would be economically feasible for a single company.

Modeling enhancements are also needed to incorporate these data into the model in a standardized way and to develop a physics-based model, which includes microstructure evolution and deformation mechanisms to describe material behavior during heat treatment. Effects of evolving microstructural features and crystallographic texture on elevated-temperature mechanical properties should be evaluated. If these are significant, a testing plan to capture theses effects should be developed. The methodology should also include aluminum airframe and nickel-based engine disk materials.

Validation: Residual stress predictions require further validation to support their quantitative application to various applications. Validation is needed on sub-scale and full-scale components in a production environment, streamlining and integration of commercial codes for user-friendly industrial implementation, and developing industry guidelines for model usage. Use cases which codify the methodology and describe the problem solving steps have been used successfully in prior programs to demonstrate the modeling framework. Standard benchmark use cases should be defined to design a heat treatment and machining process to better balance properties and distortions, and identify optimum parameters. This involves generation of experimental data under controlled and production conditions and extensive model validation followed by implementation on production hardware (Figure 44). This effort will allow comparison and transfer of residual stress predictions seamlessly through the supply-chain, including, mills, forge suppliers, OEMs, and machining suppliers.

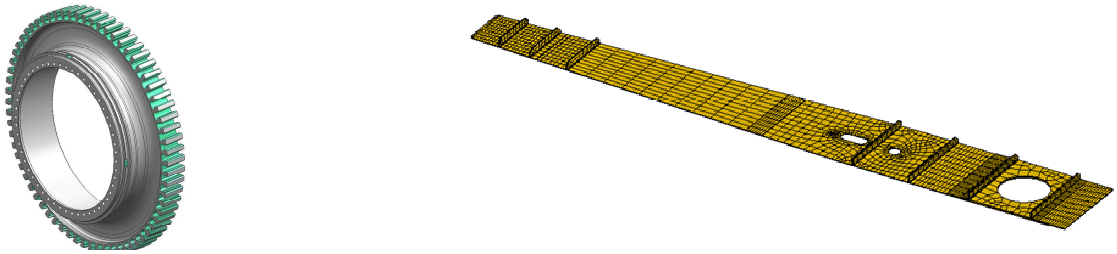

Figure 44. Typical aircraft engine and airframe applications.

Modeling sensitivity studies: Traditionally, engineering analysis is performed for nominal conditions. The design must account for various sources of uncertainty inherent in materials behavior, manufacturing processes, models, etc. to arrive at a robust control strategy to ensure minimal variability in the component characteristics. The error in residual stress predictions can be estimated by a Monte Carlo analysis driven by probability density functions that describe the uncertainty in inputs (e.g., heat transfer coefficients, material properties). An error propagation analysis should be used to quantify the compounding of errors as the analysis progresses through various steps. This will establish confidence limits on the modeling predictions and experimental measurements.

A sensitivity study is recommended to establish which inputs most strongly impact the modeling outputs of interest. Variations in the critical inputs should be quantified to assess the accuracy of the modeling outputs. Efforts can then be focused on reducing the variability in component distortion by studying the most critical steps. The sensitivity analysis can also potentially define the resolution needed in the input material property data.

Qualitative analysis is the capability to predict the trend under different processing conditions. Engineers can use this to carry out a lot of what-if studies without the need of relying on expensive experiments. Quantitative analysis is the capability to accurately predict the component behavior. This requires a accurate modeling algorithm and input parameters/data including both the boundary conditions and material properties.

Industry standards: Residual stress modeling and measurement techniques and the procedures to generate the various modeling inputs lack a standardized approach. An industry standard needs to be established that can be utilized throughout the supply-chain (mills, component producers and OEMs) to

enable integrated design, material, and processing technology efforts. As a "best practice", the analysis and experimental methods should include metrics, red flags, and/or guidelines to permit a quantitative assessment of the adequacy of each analysis and measurement. It should also include instructions about the range of applicability of the associated methods. Standards for modeling and measurement procedures, material data and boundary condition inputs should be prepared. The goal would be to develop standard methods in the form of an AMS specification. Developed "Best Practices" (input data, simulation, post-processing) should be aimed at producing consistent results, independent of the user, with acceptable accuracy.

10.0 REFERENCES

1. John Gayda, "The Effect of Heat Treatment on Residual Stress and Machining Distortions in Advanced Nickel Base Disk Alloys," NASA/TM-2001-210717.

2. Wei-Tsu Wu, Guoji Li, Juipeng Tang, Shesh Srivatsa, Ravi Shankar, Ron Wallis, Padu Ramasundaram and John Gayda, "A process modeling system for heat treatment of high temperature structural materials," Final report, USAF Contract F33615-95-C-5238, June 2001.

3. Jiann-Cherng Su, "Residual Stress Modeling In Machining Processes," Ph D Thesis, Georgia Institute of Technology, 2006.

4. McDowell, D.L. and G. J. Moyar, "A More Realistic Model of Nonlinear Material Response: Application to Elastic-Plastic Rolling Contact,". in Proceedings of the 2nd International Symposium on Contact Mechanics and Wear of Rail/Wheel Systems. 1986. Kingston, RI.

5. Gangshu Shen and David Furrer, "Manufacturing Of Aerospace Forgings," Journal of Materials Processing Technology 98 (2000) 189-195.

6. M.A. Rist, S. Tin, B.A. Roder, J.A. James, and M.R. Daymond, "Residual Stresses in a Quenched Superalloy Turbine Disc: Measurements and Modeling," Metallurgical And Materials Transactions A Volume 37a, February 2006, 459.

7. D. Dye, K.T. Conlon, and R.C. Reed, "Characterization And Modeling Of Quenching-Induced Residual Stresses In The Nickel-Based Superalloy IN718," Metallurgical And Materials Transactions A Volume 35a, June 2004, 1703.

8. T.G. Byrer (Ed), "Forging Handbook," Forging Industry Association, American Society for Metals, 1985.

9. P. J. Withers and H. K. D. H. Bhadeshia, "Overview: Residual Stress Part 1 – Measurement Techniques," Materials Science and Technology April 2001, Vol. 17, 355.

10. P. J. Withers and H. K. D. H. Bhadeshia, "Overview: Residual Stress Part 2 – Nature And Origins," Materials Science and Technology April 2001, Vol. 17, 366.

11. Timothy P. Gabb and Jack Telesman, Peter T. Kantzos, and Kenneth O'Connor, "Characterization of the Temperature Capabilities of Advanced Disk Alloy ME3," NASA/TM 2002-211796.

12. ASTM Standard E 837 – 08, "Standard Test Method for Determining Residual Stresses by the Hole-Drilling Strain-Gage Method."

13. ASTM Standard E 328 – 02 (Reapproved 2008), "Standard Test Methods for Stress Relaxation for Materials and Structures."

14. Tamas Reti, Zoltan Fried, and Imre Felde, “Computer Simulation of Steel Quenching Process using a Multi-Phase Transformation Model,” Computational Materials Science 22, 2001, 261-278.

15. Darrell Rondeau , “The Effects Of Part Orientation And Fluid Flow On Heat Transfer Around A Cylinder,” MS Thesis, Worcester Polytechnic Institute, 2004.

11.0 ACKNOWLEDGEMENTS

The authors would like to acknowledge the contributions of the team members in the various Metals Affordability Initiative (MAI) Programs: Keith Young and James Castle (Boeing); BK Chun, WT Wu, M Knezevic, and JY Oh (SFTC); Michael Glavicic and Robert Ress (Rolls-Royce); and Jeff Simmons (AFRL).